JACS
JOURNAL OF THE AMERICAN CHEMICAL SOCIETY
Article
pubs.acs.org/JACS

H_4octapa: An Acyclic Chelator for ^{111}In Radiopharmaceuticals

Eric W. Price,[†,‡] Jacqueline F. Cawthray,[†,‡] Gwendolyn A. Bailey,[†] Cara L. Ferreira,[§] Eszter Boros,[†,‡] Michael J. Adam,*[,‡] and Chris Orvig*[,†]

[†]Medicinal Inorganic Chemistry Group, Department of Chemistry, University of British Columbia, 2036 Main Mall, Vancouver, British Columbia, Canada V6T 1Z1

[‡]TRIUMF, 4004 Wesbrook Mall, Vancouver, British Columbia, Canada V6T 2A3

[§]Nordion, 4004 Wesbrook Mall, Vancouver, British Columbia, Canada V6T 2A3

Supporting Information

ABSTRACT: This preliminary investigation of the octadentate acyclic chelator H_4octapa (N_4O_4) with $^{111}In/^{115}In^{3+}$ has demonstrated it to be an improvement on the shortcomings of the current industry "gold standards" DOTA (N_4O_4) and DTPA (N_3O_5). The ability of H_4octapa to radiolabel quantitatively $^{111}InCl_3$ at ambient temperature in 10 min with specific activities as high as 2.3 mCi/nmol (97.5% radiochemical yield) is presented. In vitro mouse serum stability assays have demonstrated the ^{111}In complex of H_4octapa to have improved stability when compared to DOTA and DTPA over 24 h. Mouse biodistribution studies have shown that the radiometal complex $[^{111}In(octapa)]^-$ has exceptionally high in vivo stability over 24 h with improved clearance and stability compared to $[^{111}In(DOTA)]^-$, demonstrated by lower uptake in the kidneys, liver, and spleen at 24 h. $^1H/^{13}C$ NMR studies of the $[In(octapa)]^-$ complex revealed a 7-coordinate solution structure, which forms a single isomer and exhibits no observable fluxional behavior at ambient temperature, an improvement to the multiple isomers formed by $[In(DTPA)]^{2-}$ and $[In(DOTA)]^-$ under the same conditions. Potentiometric titrations have determined the thermodynamic formation constant of the $[In(octapa)]^-$ complex to be log K_{ML} = 26.8(1). Through the same set of analyses, the $[^{111/115}In(decapa)]^{2-}$ complex was found to have nonoptimal stability, with H_5decapa (N_5O_5) being more suitable for larger metal ions due to its higher potential denticity (e.g., lanthanides and actinides). Our initial investigations have revealed the acyclic chelator H_4octapa to be a valuable alternative to the macrocycle DOTA for use with ^{111}In, and a significant improvement to the acyclic chelator DTPA.

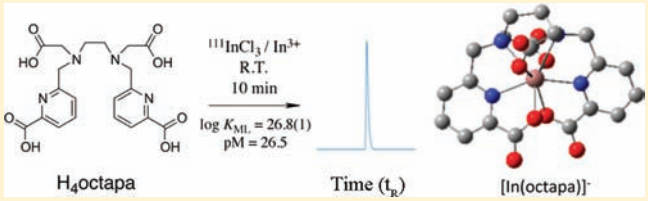

INTRODUCTION

^{111}In is an important isotope in nuclear medicine for single photon emission computed tomography (SPECT) imaging and performing dosimetry for therapeutic chelate-based radiopharmaceuticals. ^{111}In is a cyclotron-produced isotope (^{111}Cd-(p,n)^{111}In) that decays with a half-life of ~2.8 days via electron capture (100% EC); it emits γ rays (245 and 172 keV) that can be used for imaging, and Auger electrons that can be used for therapy.[1] One of the most promising radiotherapeutic isotopes, ^{90}Y ($t_{1/2}$ = ~2.67 days), is essentially radiographically silent as it only emits β^- particles, and therefore must be used in combination with an imaging isotope such as ^{111}In, ^{89}Zr, ^{86}Y, ^{64}Cu, or $^{67/68}$Ga to study its organ uptake and dosimetry.[2−4] The generator-produced indium isotope ^{110m}In ($t_{1/2}$ = 69 min) is a very attractive positron emission tomography (PET) imaging surrogate for ^{111}In, and the two isotopes can be seamlessly interchanged in bifunctional-chelate (BFC)-based radiopharmaceuticals because they share identical chemical properties.[5] When used with the OctreoScan kit, ^{110m}In has been shown to significantly improve spatial resolution, dosimetry, and tumor identification when compared to ^{111}In;[5] however, the generator parent isotope ^{110}Sn has a half-life of ~4.1 h, which makes the generator life very short.[6]

There are currently several $^{111}In/^{90}Y$-based radiopharmaceuticals FDA-approved for clinical use and many more in clinical trials, demonstrating the importance of these isotopes in nuclear medicine.[7−13] The combination of ^{111}In for imaging and dosimetry and $^{90}Y/^{177}$Lu for therapy is very effective but is dependent on having a solid chelator foundation that can bind both isotopes with exceptionally high stability (thermodynamic and kinetic) and that has very similar biological behavior with both isotopes (biologically equivalent).[14−21] The macrocycle DOTA (1,4,7,10-tetraazacyclododecane-1,4,7,10-tetraacetic acid) is the industry "gold standard" for chelation of ^{111}In, ^{90}Y, and ^{177}Lu (Chart 1); however, biovector conjugates suffer from the need for elevated temperatures and extended reaction times to achieve quantitative radiolabeling yields (typically 60−95 °C, for 30−120 min), which is not optimal for use with heat-sensitive biomolecules like antibodies.[22−25] Peptide biovectors can often be labeled at elevated temperatures without suffering deleterious effects to their binding integrity and have also shown excellent tumor targeting and uptake; however, with the current chelator offerings they sometimes demonstrate high

Received: March 13, 2012
Published: April 29, 2012

   dx.doi.org/10.1021/ja3024725 | J. Am. Chem. Soc. 2012, 134, 8670−8683

Chart 1. Structures of the ^{111}In-Coordinating and Industry "Gold Standard" Chelators DTPA/CHX-A″-DTPA and DOTA, the ^{68}Ga-Coordinating Chelator H_2dedpa, and the Novel Entrants H_4octapa and H_5decapa

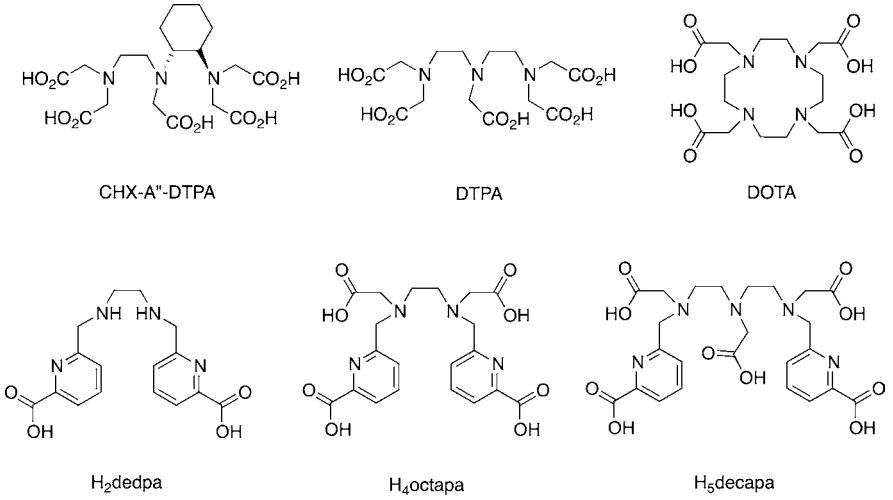

and persistent kidney uptake that can disrupt the predictive power of dosimetry calculations and cause unwanted radiation exposure.[20,26]

Since the properties of the radiometal−chelate complex can strongly influence the biodistribution profile of its peptide conjugate, a new chelator with an improved clearance profile and decreased persistent kidney uptake would be a welcome improvement. Although the influence of chelate properties on the biodistribution of BFC conjugates is less significant for large biovectors like antibodies (∼150 kDa for an intact antibody) than it is for smaller peptides, the difference can still be significant.[2,20,21] Antibody biovectors show exceptionally high tumor uptake and have long biological half-lives (2−3 weeks[27]), and thus are well matched with the long half-lives of ^{90}Y (∼2.67 days) and ^{177}Lu (∼6.6 days).[1] The acyclic chelator DTPA (diethylenetriamine tetraacetic acid) will successfully radiolabel these isotopes in 10−15 min at ambient temperature; however, the in vivo stability is less than optimal, showing a greater extent of decomposition and nontarget organ uptake than DOTA.[20,28−30] The DTPA derivative CHX-A″-DTPA has an improved stability profile with $^{86/90}$Y when compared to DTPA, while retaining its low-temperature labeling abilities; however, the stability and in vivo kinetic inertness are still not as good as DOTA, and its In^{3+} complexes have been less studied.[28−32] Despite the poor in vivo stability, DTPA is the chelator used in the currently available FDA approved ^{111}In-based radiopharmaceuticals.

Our group has recently investigated a series of acyclic chelators, resulting in identification of the promising $^{67/68}$Ga chelator H_2dedpa (Chart 1).[33,34] Initial radiolabeling experiments, in vitro apo-transferrin stability experiments, and biodistribution studies in mice have demonstrated H_2dedpa to be an ideal chelator for $^{67/68}$Ga-based radiopharmaceuticals.[35] This success has prompted the investigation of larger acyclic frameworks based on the basic H_2dedpa scaffold, supporting higher denticities for accommodating larger radiometal ions such as ^{111}In, ^{90}Y, ^{177}Lu, ^{89}Zr, and ^{225}Ac. Herein we report the synthesis, characterization, coordination chemistry, thermodynamic stability, radiolabeling, in vitro mouse serum stability, and in vivo biodistribution studies of the ^{111}In complexes of the previously reported but uniquely applied octadentate chelator *N*,*N*′-bis(6-carboxy-2-pyridylmethyl)ethylenediamine-*N*,*N*′-diacetic acid (referred to herein as H_4octapa) (Chart 1),[36] and the novel decadentate derivative H_5decapa. DOTA and DTPA were used as benchmarks of the industry "gold standards" for ^{111}In chelation.

RESULTS AND DISCUSSION

Although the macrocycle DOTA is the most stable chelator for ^{111}In, it is essentially incompatible with antibodies due to its required high-temperature radiolabeling, and the excellent match of antibodies with long-lived therapeutic isotopes makes this mismatch especially unfortunate. This suggests an important and high-priority need for new, highly stable acyclic chelators for use with isotopes such as ^{111}In, ^{90}Y, and ^{177}Lu, especially when conjugated to antibodies. There is a need for chelators that combine the exceptional in vivo stability and kinetic inertness of DOTA with the fast ambient temperature labeling kinetics of DTPA. These observations suggest that the target for an ideal ^{111}In/^{90}Y/^{177}Lu chelator would have the following properties. It should (1) be acyclic or if macrocyclic, be constructed with free-moving appendages to emulate the low-temperature acyclic radiolabeling kinetics, such as that of BCNOTA.[37] The coordination complex should (2) be very stable, both thermodynamically and kinetically, but with top priority placed on exceptional in vivo kinetic inertness, particularly to demetalation and/or transchelation. The coordination complex should (3) exhibit minimal isomerization and fluxional behavior, and the chelator should be isomerically pure with preferably only one stable isomer being formed and administered or, like CHX-A″-DTPA, the superior isomer of the chelator isolated and administered pure.[28−30] Finally, it should (4) ideally have similar properties in its chelate/bifunctional-chelate complexes with both of the radiometal ions to be used in an imaging/therapy pair (i.e., ^{111}In/^{90}Y), so that biological clearances and organ uptakes are sufficiently similar and that accurate dosimetry information can be obtained (bioequivalence). Not every one of these four points must be met for a chelator to be useful as a BFC for radiometal ions, and especially point number four may be hard to achieve, considering the different coordination numbers and geometries preferred by different metal ions such as ^{111}In (6−8 coordinate) and ^{90}Y (8−9 coordinate).[38]

dx.doi.org/10.1021/ja3024725 | J. Am. Chem. Soc. 2012, 134, 8670−8683

Scheme 1. Synthesis of Compounds 1, 2, 3, 4, 5, 6, and H_4octapa[a]

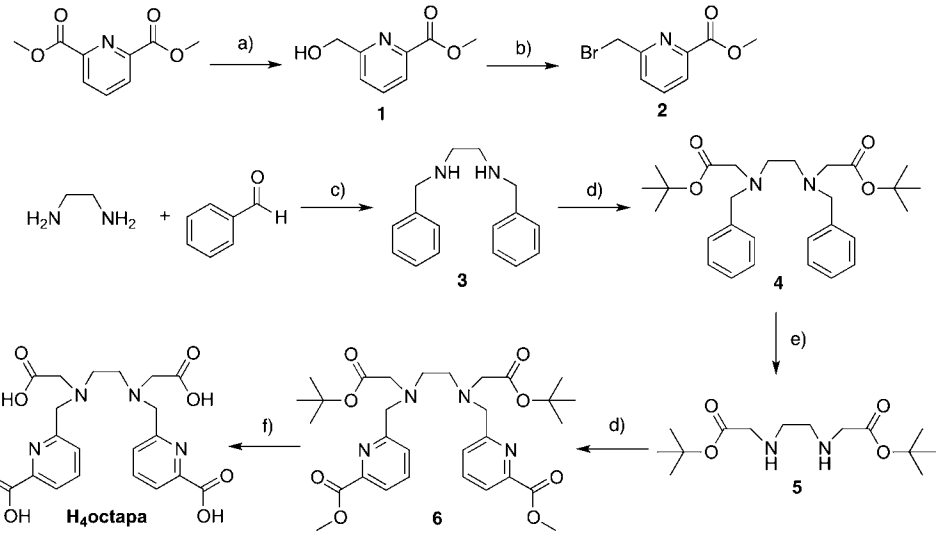

[a]Reagents and conditions: a) $NaBH_4$ (2.4 equiv), CH_3OH, 4 h, 0 °C, 51%; b) PBr_3 (1.1 equiv), $CHCl_3$, 0 °C, 3.5 h, 99%; c) CH_3OH, $NaBH_4$ (4.3 equiv), 8 h, 49%; d) CH_3CN, Na_2CO_3 (excess), 60 °C, Ar (g), 12−16 h, **4** = alkylation with *tert*-butyl bromoacetate, 93%, **6** = alkylation with **2**, 39%; e) AcOH, Pd/C (10 wt %), H_2 (g), 12 h, 87%; f) HCl (6 M), Δ 8 h, 75%.

Scheme 2. Synthesis of Compounds 7, 8, 9, 10, and H_5decapa[a]

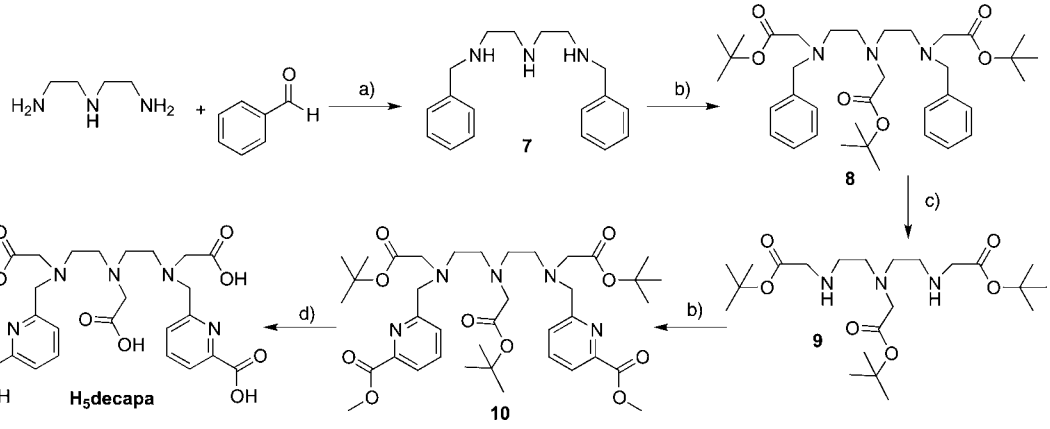

[a]Reagents and conditions: a) CH_3OH, $NaBH_4$ (7 equiv), 8 h, 40%; b) CH_3CN, Na_2CO_3 (excess), 60 °C, Ar (g), 12−16 h, **8** = alkylation with *tert*-butyl bromoacetate, 66%, **10** = alkylation with **2**, 45%; c) AcOH, Pd/C (5 wt %), H_2 (g), 12 h, 30%; d) HCl (6 M), Δ 8 h, 71%.

Synthesis and Characterization. We have studied a number of novel acyclic chelators, and herein we report our two most promising candidates for use with ^{111}In. The previously reported, but here uniquely applied, octadentate chelator *N*,*N*′-bis(6-carboxy-2-pyridylmethyl)ethylenediamine-*N*,*N*′-diacetic acid (H_4octapa) was previously used with various paramagnetic lanthanides to assess their abilities as MRI contrast agents.[36] As an expansion of this scaffold, the novel decadentate derivative H_5decapa has also been synthesized and evaluated. The chelators H_4octapa and H_5decapa were synthesized with a general reaction scheme that follows *N*-benzyl protection, *N*-alkylation with an alkyl halide, benzyl deprotection via hydrogenation, a second alkyl halide *N*-alkylation, and finally deprotection in refluxing HCl (6 M) (Schemes 1 and 2). Previous methods to synthesize the similar acyclic chelator H_2dedpa utilized reductive amination reactions;[33,36] however, this method resulted not only in reduction of the imines but also reduction of the picolinic acid methyl ester groups to carboxylates and alcohols, which were very difficult to separate in subsequent steps, resulting in low purified yields. The synthetic scheme presented here circumvents this problem by avoiding the use of sodium borohydride in the presence of the picolinic acid moiety (Schemes 1 and 2). The only significant problem encountered with these syntheses is the lability of the picolinate groups to hydrogenation. Benzylated intermediates that contain picolinate groups undergo unwanted cleavage during hydrogenation, and to minimize this undesirable pathway the reaction order was optimized to perform the debenzylation step only in the presence of the *tert*-butylacetate groups (Schemes 1 and 2). The obvious drawback to this method is that after hydrogenation, the *tert*-butylacetate-alkylated ethylenediamine/diethylenetriamine compounds (**5**/**9**) are not UV active and must be stained with iodine to be visualized. Hydrogenation of the diethylenetriamine scaffold during the synthesis of H_5decapa resulted in substantial cleavage of the diethylenetriamine backbone, resulting in lower yields than the equivalent hydrogenation of the ethylenediamine scaffold in the H_4octapa synthesis. Decreasing

dx.doi.org/10.1021/ja3024725 | J. Am. Chem. Soc. 2012, 134, 8670−8683

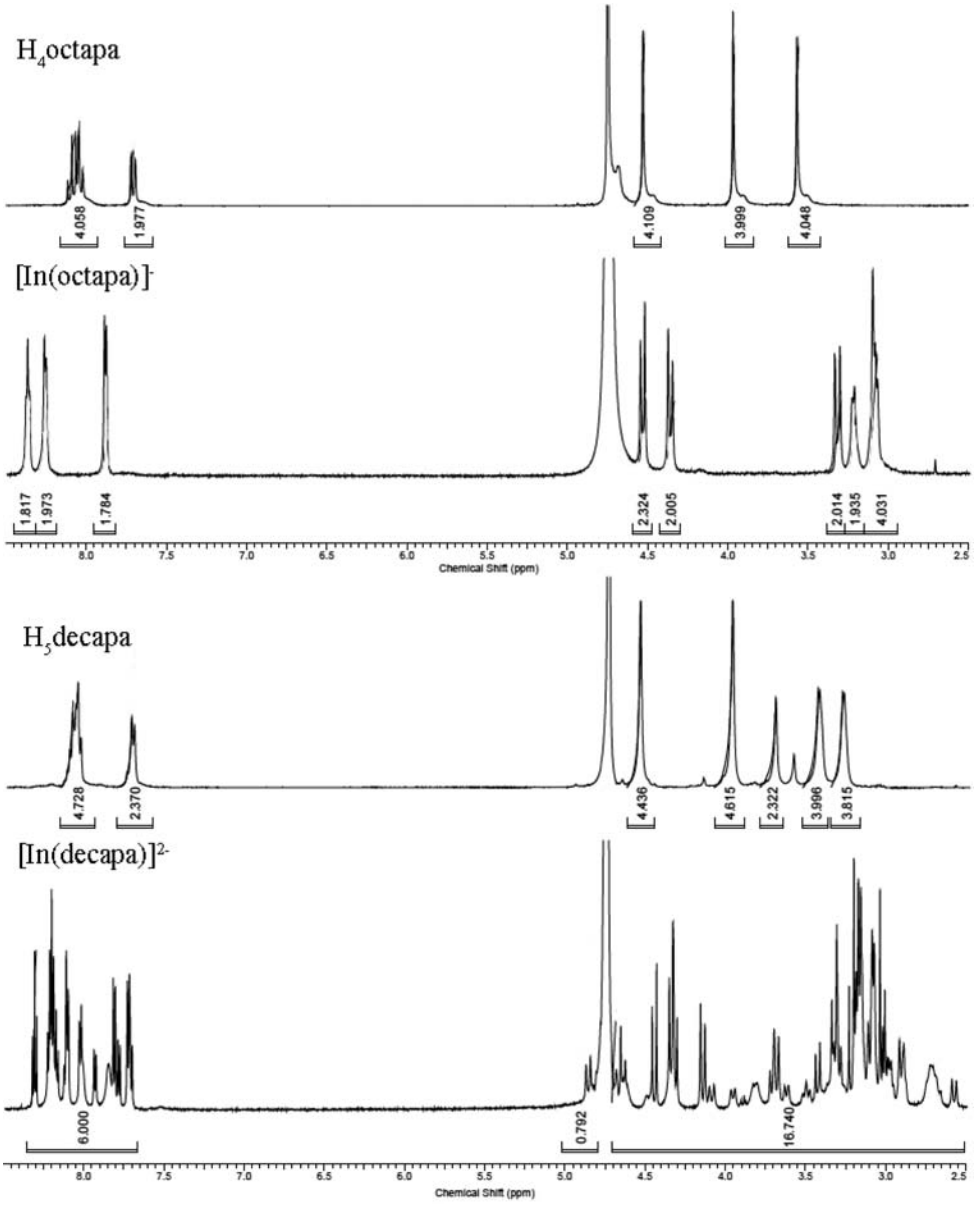

Figure 1. ^{1}H NMR spectra in D_2O at ambient temperature of (top) H_4octapa (300 MHz) and $[In(octapa)]^-$ (600 MHz) showing simple diastereotopic splitting due to minimal isomerization and (bottom) H_5decapa (400 MHz) and $[In(decapa)]^{2-}$ (600 MHz) showing complicated splitting arising from multiple isomers.

the Pd/C catalyst loading appeared to slow down reaction kinetics and did not improve selectivity for debenzylation over the unwanted side reactions.

The presented synthetic schemes are an obvious improvement over previous attempts, allowing for improved yields and the purification of all intermediates despite the large number of polar functional groups; however, the problem of nonselective debenzylation and ethylene backbone cleavage of diethylenetriamine is problematic, and with larger scaffolds such as tris(2-aminoethyl)amine (TREN) this problem becomes more severe. These challenges suggest that new protecting-group chemistry must be employed to further improve the synthesis of these picolinic acid-based chelators and facilitate the elaboration of larger scaffolds and novel bifunctional derivatives. The relatively simple five-step synthesis of H_4octapa is achieved with a cumulative yield of ∼12%, and the five-step synthesis of H_5decapa was completed with a cumulative yield of ∼2.5% (yields for both compounds using previous methods were under 1%). The incorporation of multiple synthons in the synthesis of these chelators will allow for more straightforward syntheses of bifunctional derivatives via (4-nitrobenzyl)-ethylenediamine/diethylenetriamine backbone derivatives, which should be an improvement over the difficult and tedious synthesis of bifunctional macrocycles like *p*-isothiocyanatobenzyl DOTA.[39]

In general, chelates/BFC that exhibit minimal isomerization are preferred and tend to be more stable in vivo.[40−42] The ^{1}H NMR spectrum of $[In(octapa)]^-$ showed clear and sharply resolved diastereotopic splitting of the protons associated with both picolinic acid moieties (methylene-*H*, 4.49 ppm, ^{2}J = 16.1 Hz, and 4.34 ppm, ^{2}J = 16.1 Hz), as well as one of the acetic acid arms (3.27 ppm, ^{2}J = 19.3 Hz), suggesting a 7-coordinate solution structure (Figure 1). The coupling constants observed for these metal-bound appendages were ^{2}J = 16.1 Hz for the

dx.doi.org/10.1021/ja3024725 | J. Am. Chem. Soc. 2012, 134, 8670−8683

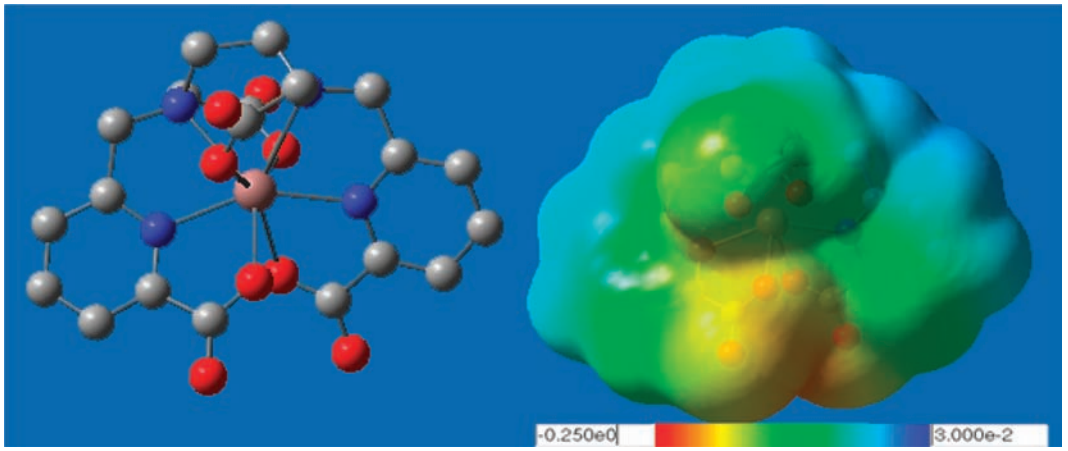

Figure 2. DFT structure of $[In(octapa)]^-$ (solvent = water) showing an 8-coordinate structure (left), and the electrostatic potentials of the complex between $octapa^{4-}$ with In^{3+} mapped onto the electron density (right). The MEP represents a maximum potential of 0.03 au, and a minimum of −0.25 au, mapped onto electron density isosurfaces of 0.002 e $Å^{-3}$ (red to blue = negative to positive).

two picolinic acid methylene groups, and ^2J = 19.3 Hz for the acetic acid arm. The second acetic acid arm appeared as a broad doublet (3.19 ppm) with a much smaller coupling constant of ^2J = 8.4 Hz, showing diasterotopic splitting but suggesting it is not metal-bound and does not form a five-membered metallocycle like the other metal-bound appendages. The sharp and clear diasterotopic splitting seen for $[In(octapa)]^-$ suggests the presence of a single isomer with no observable fluxional interconversion at ambient temperature (on the NMR time scale). No change in the number of peaks in the ^{13}C NMR spectrum of the ligand H_4octapa was observed upon In^{3+} coordination, suggesting no chemically distinct isomers were formed (different coordination number/polarity) (Figure S8, Supporting Information [SI]). The HPLC radiotrace of $[In(octapa)]^-$ showed a single sharp peak, affirming that the radiometal complex exhibits minimal isomerization (Figure S19 [SI]). This reveals a very stable and inert coordination structure present as a single isomer, unlike the $[In(DOTA)]^-$ complex which shows multiple isomers with rapid fluxional isomerization at ambient temperature.[42,43]

The In^{3+} complex formed with the potentially decadentate chelator H_5decapa, $[In(decapa)]^{2-}$, displayed a more complex ^1H NMR splitting (Figure 1) and a large number of additional ^{13}C NMR peaks that were not observed for the free ligand H_5decapa (Figures S12, S14, SI). This observation, along with the presence of two peaks in the HPLC radiotrace (t_R = 5.4 min (5%), 7.7 min (95%), Figure S20 [SI]) suggests that multiple isomers (including chemically distinct isomers) of $[In(decapa)]^{2-}$ are present in solution at ambient temperature. Considering that In^{3+} typically forms 7−8-coordinate complexes, the decadentate chelator H_5decapa may have several unbound carboxylates, which could give rise to different protonation species in solution and could explain the two peaks observed in the HPLC radiotrace. Additionally, NMR experiments (D_2O) and HPLC experiments were performed at different pH, which could influence the protonation species present in solution. $[In(DTPA)]^{2-}$ displays a complicated splitting of the ^1H NMR peaks in a similar fashion to $[In(decapa)]^{2-}$, and also yields sharp splitting patterns suggesting that little or no fluxional behavior between multiple isomers/diastereomers occurs in solution at ambient temperature.[44,45] Unlike $[In(decapa)]^{2-}$, $[In(DTPA)]^{2-}$ retains a simple ^{13}C NMR spectrum with no additional peaks to the free ligand.[44] These observations for $[^{111}In(DTPA)]^{2-}$ suggest that little or no fluxional behavior between isomers/diastereomers occurs in solution at ambient temperature (on the NMR time scale), although multiple isomers are indeed formed.[42,44,45] If minimal isomerization and fluxional behavior are optimal for stability,[40−42] then the NMR solution structures of the currently investigated In^{3+} chelator complexes would have them ranked as $[In(octapa)]^-$ > $[^{111}In(DTPA)]^{2-}$ > $[In(DOTA)]^-$ > $[In(decapa)]^{2-}$. As previously discussed, DTPA has been shown to be inferior to DOTA in terms of in vivo stability with In^{3+} and so does not fit with this trend; however, this work largely follows the trend with the in vivo stability of H_4octapa being superior to DOTA, and H_5decapa being inferior to both.

The ^1H NMR spectrum of the hexadentate $[In(dedpa)]^+$ complex in D_2O was very similar to that of $[In(octapa)]^+$, and showed a sharp doublet for each set of methylene protons (4.58 ppm, ^2J = 17.3 Hz, and 4.13 ppm, ^2J = 17.4 Hz) associated with the picolinic acid moiety (Figure S26 [SI]). The ^1H NMR spectrum of the hexadentate $[In(dedpa)]^+$ complex in DMSO-d_6 revealed two sharp doublets for each set of methylene protons (4.27 ppm, ^2J = 16.6 Hz, 4.26 ppm, ^2J = 16.3 Hz, 3.90 ppm, ^2J = 16.6 Hz. 3.89 ppm, ^2J = 16.6 Hz) attached to the picolinic acid moieties, suggesting clean diastereotopic splitting arising from two separate isomers, most likely from DMSO binding to the open coordination sites of In^{3+} (Figure S26 [SI]). The sharp peaks observed for $[In(dedpa)]^+$ in D_2O and DMSO-d_6 suggest no observable fluxional behavior at ambient temperature, and the presence of only one set of peaks in the ^{13}C NMR spectrum (same as unbound H_2dedpa, Figures S16 and S18 [SI]) and one peak in the HPLC radiotrace (vide infra) suggests the formation of only one isomer. In consideration of these results, the very simple and sharp diastereotopic proton splitting observed in the ^1H NMR spectrum of $[In(octapa)]^-$, coupled with the single sharp peak observed in the HPLC radiotrace, suggests that this complex displays the least amount of isomerization and fluxional behavior in solution at ambient temperature out of the currently investigated novel chelators and the industry "gold standards" DTPA and DOTA.

DFT Structures and Molecular Electrostatic Potential Maps. Although solid-state structures of metal−chelate complexes obtained from X-ray crystallography are useful,

dx.doi.org/10.1021/ja3024725 | J. Am. Chem. Soc. 2012, 134, 8670−8683

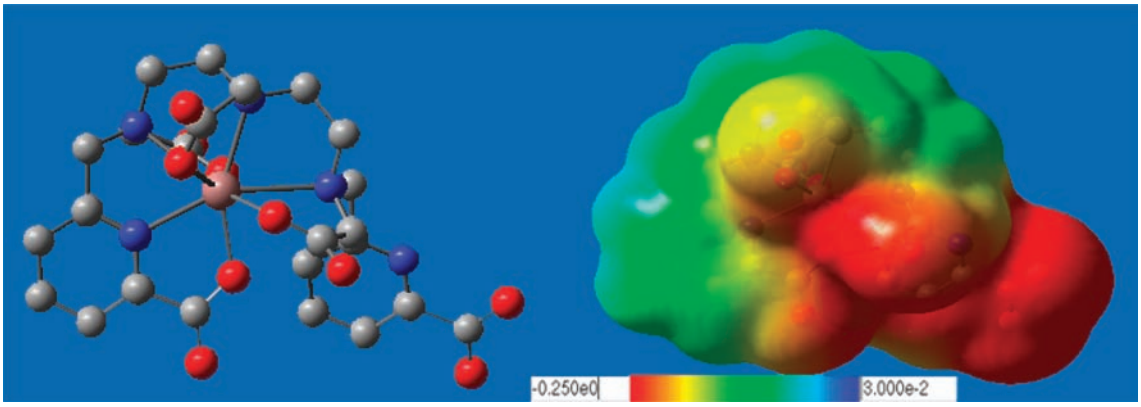

Figure 3. DFT structure of $[In(decapa)]^{2-}$ (solvent = water) showing an 8-coordinate structure, with one picolinic acid group unbound and extended away from the metal center (left), and the electrostatic potentials of the complex between $decapa^{5-}$ with In^{3+} mapped onto the electron density (right). The MEP represents a maximum potential of 0.03 au, and a minimum of −0.25 au, mapped onto electron density isosurfaces of 0.002 e $Å^{-3}$ (red to blue = negative to positive).

they are often not representative of the solution-phase structures, and so DFT calculations (modeled in water) and NMR studies in D_2O of solution structures are most relevant to a discussion of potential in vivo applications.[38,42,46] The DFT structure of $[In(octapa)]^-$ (Figure 2, left) reveals an 8-coordinate complex with approximately C_{2v} symmetry, showing tight binding of In^{3+} with slight puckering of the picolinic acid moieties. The solution structure of $[In(octapa)]^-$ as deduced by NMR spectroscopy suggests a 7-coordinate structure with one acetic acid arm unbound; however, it is not certain from the broad doublet (3.22 ppm) and smaller coupling constant (8.4 Hz) of the unbound acetic acid arm whether or not there is transient metal binding. The DFT structure of $[In(decapa)]^{2-}$ (Figure 3, left) shows an 8-coordinate structure, with one picolinic acid and all three acetic acid arms bound to indium (as well as the three tertiary backbone nitrogen atoms), and one picolinic acid group unbound and extended away from the metal center. This unsymmetric coordination sphere has a large impact on the electrostatic potential of the complex (Figure 3, right), with the MEP map revealing the entire molecular surface to be more electronegative than $[In(octapa)]^-$ (Figure 2, right). $[In(decapa)]^{2-}$ shows areas of very high electronegative potential around the unbound picolinic acid group, most likely from the unbound deprotonated carboxylate group (Figure 3, right). The unsymmetric high density of electronegative potential shown on the MEP map of $[In(decapa)]^{2-}$, in contrast to the symmetric and less electronegative charge distribution of $[In(octapa)]^-$, may result in a higher propensity toward protonation and protein binding in vivo, and may be partially responsible for the poor stability in vivo.

Radiolabeling Experiments. Initial radiolabeling experiments demonstrated the ability of H_4octapa to radiolabel quantitatively ^{111}In at ambient temperature in 10 min, showing a single sharp peak in the HPLC radiotrace at t_R = 4.7 min (Figure S27, SI). Radiolabeling with $[In(octapa)]^-$ yields specific activities as high as 2.3 mCi/nmol (~5 mCi/μg, 2300 mCi/μmol) in 10 min at ambient temperature. DOTA was radiolabeled with the same activity of ^{111}In (~1 mCi) at the same ligand concentration (10^{-7} M) used to obtain the specific activity listed above for $[In(octapa)]^-$, after 10 min at ambient temperature less than 40% ^{111}In was radiometalated. This demonstrates the ability of H_4octapa to radiolabel ^{111}In quantitatively and rapidly in high specific activities at ambient temperature, which is in sharp contrast to the "gold standard" DOTA. The theoretical maximum ^{111}In specific activity has been calculated to be ~46 mCi/nmol, and specific activities as high as 22 mCi/nmol have been reported for ^{111}In-labeled DOTA−peptide conjugates under ideal conditions; however, temperatures of 100 °C for 30 min were required, and specific activities that high are not typical with DOTA-conjugates.[47] To compare recently reported examples, a ^{111}In-CHX-A″-DTPA−Re(Arg11)CCMSH peptide conjugate yielded a specific activity of ~0.29 mCi/nmol,[48] DTPA−(gp100:154−162mod) (HLA-A2.1 binding peptide conjugate) showed a maximum specific activity of ~0.35 mCi/nmol,[49] and a DOTA−RGD conjugate obtained a specific activity as high as ~0.050 mCi/nmol;[50] these are more typical values and are much lower than the ~2.3 mCi/nmol specific activity obtained for $[In(octapa)]^-$ during this study. It must be considered, however, that the examples listed above are for chelator−peptide conjugates, and the values obtained in this study were for nonconjugated $[In(octapa)]^-$. DOTA−biovector conjugates typically offer lower specific activities when compared to acyclic chelators such as DTPA and CHX-A″-DTPA.[48] The HPLC radiotrace of $[In(decapa)]^{2-}$ was less promising and revealed two peaks (t_R = 5.4 min (5%), 7.7 min (95%)), possibly due to multiple chemically distinct isomers being formed, with specific activities being low at ~0.030 mCi/nmol. As previously discussed, DOTA required temperatures of 80 °C in a microwave reactor for ~20 min to label ^{111}In.

Thermodynamic Stability. Formation constants (log K_{ML}) are well-established measurements of thermodynamic stability for metal−ligand complexes and are typically reported in the literature; however, pM ($-\log[M^{n+}_{free}]$) values are much more accurate figures for predicting in vivo thermodynamic stability under physiologically relevant conditions. Values of pM are calculated (at specific conditions, here $[M^{n+}]$ = 1 μM, $[L^{x-}]$ = 10 μM) to take into account all of ligand basicity (ligand pK_a values), free metal concentration, ligand-to-metal ratios, pH, and metal hydroxide formation. The thermodynamic stability of $[In(octapa)]^-$ was determined to be log K_{ML} = 26.8(1) (pM = 26.5), which is significantly higher than that for DOTA (log K_{ML} = 23.9(1), pM = 18.8) and similar to DTPA (log K_{ML} = 29.0, pM = 25.7) but shows the highest pM value of all three In^{3+} complexes (Table 1). Although CHX-A″-DTPA has been evaluated with Y^{3+} to be very stable,[51] it has not been thoroughly studied with In^{3+} and to our knowledge formation constants have not yet been reported. Despite $[In(DOTA)]^-$

dx.doi.org/10.1021/ja3024725 | J. Am. Chem. Soc. 2012, 134, 8670−8683

Table 1. Formation Constants (log K_{ML}) and pM[a] Values for In^{3+} Complexes

chelator	log K_{ML}	pM[a]
dedpa^{2-}	26.60(4)	25.9
octapa^{4-}	26.8(1)	26.5
decapa^{5-}	27.56(5)	23.1
oxine (tris)[53]	35.4	34.1
DTPA[52,53]	29.0	25.7
DOTA[53,54]	23.9(1)	18.8
transferrin[55]	18.3	18.7

[a]Calculated for 10 μM total ligand and 1 μM total metal at pH 7.4 and 25 °C.

being significantly more stable in vivo than is [In(DTPA)],[2−20,28−30] the log K_{ML} and pM values are much lower for DOTA than for DTPA with In^{3+}. It is interesting to note that the trend of stability constants (log K_{ML}) and pM values in Table 1 do not correlate well with in vivo stability, which emphasizes that these thermodynamic parameters are not the only factors involved in determining biological stability. The kinetic parameters of ligand−metal on/off rates are the most important factor, with $[In(DOTA)]^-$ having one of the lowest pM values and very high stability/kinetic inertness in vivo, and with $In(oxine)_3$ having the highest log K_{ML} and pM values (log K_{ML} = 35.3, pM = 34.1) and dissociating very quickly in vivo.[13] These values reinforce the concept that in vitro competition experiments such as mouse serum and apo-transferrin competitions, and in vivo biodistribution and stability studies are essential to evaluate the practical in vivo kinetic inertness and metabolism of radiometal complexes. Because the thermodynamic formation constants of the H_4octapa, H_5decapa, and H_2dedpa ligands with In^{3+} are all very similar, the large differences in pM values must be a result of ligand basicity. Despite these complications, it is encouraging that $[In(octapa)]^-$ has an exceptionally high pM value of 26.5, which is higher than the values previously for determined DOTA (18.8) and DTPA (25.7) with In^{3+}.[52−54]

Stability Studies. In consideration of the fact that in vivo kinetic inertness plays a crucial role in determining stability, competition experiments using native biological chelators such as those contained in blood serum (e.g., apo-transferrin, albumin) are useful in vitro assays for predicting the in vivo stability and kinetic inertness of radiometal ion complexes. During preliminary experiments, mouse serum stability assays were found to show transchelation of In^{3+} more aggressively than were apo-transferrin assays. These mouse serum competition experiments (incubated at ambient temperature) have demonstrated $[In(octapa)]^-$ to have marginally higher stability than $[In(DOTA)]^-$ and $[In(DTPA)]^{2-}$ after 24 h, within error (92.3 ± 0.04%, 89.4 ± 2.2%, 88.3 ± 2.2%, respectively) (Table 2). $[In(decapa)]^{2-}$ also demonstrated exceptional stability against mouse serum transchelation with a stability of 89.1 ± 1.7% at 24 h.

Mouse biodistribution studies were performed with $[^{111}In(octapa)]^-$, $[^{111}In(DOTA)]^-$, and $[^{111}In(decapa)]^{2-}$, and the data summarized in Figure 4 (*y*-axis adjusted to 2% injected dose (ID)/g for visualization of 4 and 24 h time points) shows rapid clearance through the kidneys for $[^{111}In(octapa)]^-$ and $[^{111}In(DOTA)]^-$, with activity clearing quickly from all organs. The clearance of $[^{111}In(decapa)]^{2-}$ is not as rapid, with ^{111}In levels slowly increasing over 24 h in the liver, spleen, and bone (Table 3). These results are typical of a metal−ligand complex

Table 2. Data from Mouse Serum Stability Challenges Performed at Ambient Temperature (n = 3), with Stability Shown As the Percentage of Intact ^{111}In Complex

complex	1 h stability (%)	24 h stability (%)
$[^{111}In(dedpa)]^+$	96.1 ± 0.1	19.7 ± 1.5
$[^{111}In(octapa)]^-$	93.8 ± 3.6	92.3 ± 0.04
$[^{111}In(decapa)]^{2-}$	89.7 ± 1.6	89.1 ± 1.7
$[^{111}In(DOTA)]^-$	89.6 ± 2.1	89.4 ± 2.2
$[^{111}In(DTPA)]^{2-}$	86.5 ± 2.2	88.3 ± 2.2

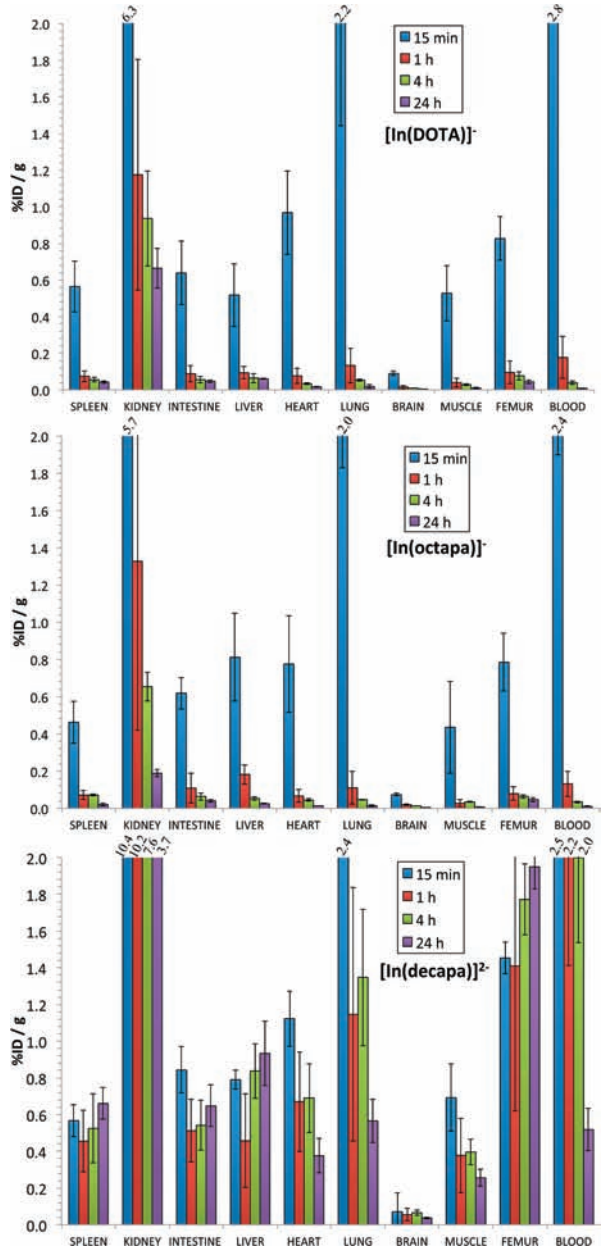

Figure 4. Biodistribution % ID/g values for $[^{111}In(DOTA)]^-$, $[^{111}In(octapa)]^-$, and $[^{111}In(decapa)]^{2-}$, with error bars plotted as standard deviations (note the *y*-axis set to 2.0% ID/g, for clarity of the low activity 4 and 24 h time points).

that is unstable in vivo and undergoes demetalation/transchelation, which is surprising because of the high degree of stability of $[^{111}In(decapa)]^{2-}$ in mouse serum competition experiments (Table 2). The most promising result from these

dx.doi.org/10.1021/ja3024725 | J. Am. Chem. Soc. 2012, 134, 8670−8683

Table 3. Decay-Corrected % ID/g Values from the Biodistribution of ^{111}In-Complexes in Healthy Female ICR Mice (6-8 weeks old), n = 4, bold = Passed Student's T-Test ($p < 0.05$)

organ	15 min	SD	1 h	SD	4 h	SD	24 h	SD
				$[^{111}In(DOTA)]^-$				
spleen	0.564	0.140	0.074	0.030	**0.054**	0.013	**0.043**	0.007
kidney	6.275	3.652	1.175	0.631	0.935	0.259	**0.664**	0.108
intestine	0.638	0.173	0.088	0.047	0.055	0.019	0.047	0.008
liver	0.518	0.172	0.093	0.033	0.064	0.025	**0.061**	0.002
heart	0.967	0.228	0.077	0.042	**0.034**	0.005	0.017	0.004
lung	2.218	0.776	0.134	0.095	0.053	0.007	0.018	0.009
brain	0.090	0.013	0.015	0.010	**0.010**	0.001	0.001	0.0005
muscle	0.527	0.152	0.040	0.025	0.028	0.005	0.010	0.004
femur	0.826	0.119	0.095	0.063	0.077	0.023	0.044	0.011
blood	2.768	0.536	0.177	0.116	0.038	0.008	0.008	0.002
urine	306.197	120.471	523.638	542.402	3.726	3.643	0.131	0.069
				$[^{111}In(octapa)]^-$				
spleen	0.462	0.113	0.072	0.024	0.072	0.004	**0.020**	0.008
kidney	5.738	1.027	1.327	0.907	0.654	0.078	**0.189**	0.019
intestine	0.619	0.085	0.109	0.080	0.064	0.020	0.041	0.007
liver	0.811	0.235	0.182	0.051	0.053	0.009	**0.025**	0.003
heart	0.775	0.259	0.066	0.033	**0.045**	0.006	0.014	0.002
lung	2.003	0.175	0.111	0.088	0.047	0.003	0.014	0.007
brain	0.073	0.008	0.019	0.004	**0.014**	0.001	0.003	0.002
muscle	0.435	0.248	0.028	0.019	0.034	0.003	0.007	0.002
femur	0.785	0.154	0.079	0.035	0.064	0.009	0.047	0.012
blood	2.422	0.523	0.132	0.068	0.035	0.005	0.010	0.002
urine	506.246	146.573	229.086	200.871	5.961	5.761	0.124	0.045
				$[^{111}In(decapa)]^{2-}$				
spleen	0.567	0.049	0.455	0.170	0.525	0.187	0.661	0.085
kidney	10.380	2.095	10.210	2.835	7.554	0.928	3.681	0.539
intestine	0.843	0.107	0.513	0.172	0.541	0.136	0.647	0.113
liver	0.790	0.040	0.457	0.255	0.838	0.149	0.934	0.175
heart	1.123	0.170	0.671	0.272	0.691	0.188	0.376	0.093
lung	2.375	0.082	1.146	0.691	1.347	0.373	0.566	0.117
brain	0.071	0.007	0.055	0.033	0.065	0.014	0.036	0.004
muscle	0.692	0.126	0.378	0.203	0.396	0.070	0.256	0.045
femur	1.453	0.124	1.410	0.790	1.772	0.193	1.950	0.121
blood	2.456	0.980	2.207	0.795	1.999	0.463	0.518	0.115
urine	318.209	91.598	53.949	13.363	60.685	66.949	0.666	0.513

animal experiments is that the radiometal complex $[^{111}In(octapa)]^-$ has exceptional in vivo stability over 24 h, with improved clearance compared to $[^{111}In(DOTA)]^-$ (Figure 4), most notably from the kidneys (0.189 ± 0.019% ID/g vs 0.664 ± 0.108% ID/g, respectively, Figure S23 [SI]), liver (0.0248 ± 0.0030% ID/g vs 0.0605 ± 0.0022% ID/g, respectively, Figure S24 [SI]), and spleen (0.0202 ± 0.0083% ID/g vs 0.0426 ± 0.0067% ID/g, respectively, Figure S25 [SI]) at 24 h ($p < 0.05$, Table S4 [SI]). These findings are significant because in vivo instability resulting in demetalation or transchelation via serum proteins typically results in high uptake of "free" ^{111}In in the liver, spleen, bone, and kidneys (typical of transferrin-bound 3^+ metals), with levels increasing over time.[56] Surprisingly, despite the exceptional mouse serum stability of $[In(decapa)]^{2-}$, the in vivo stability in mice was found to be suboptimal, with slower clearance from the blood pool and most notably high persistent kidney (3.68 ± 0.54% ID/g) and increasing bone uptake (1.95 ± 0.12% ID/g) over 24 h; however, all other organs contained less than 1% ID/g after 24 h (Figure 4, Table 3). Although these values are inadequate when compared to the in vivo stability and clearance of exceptionally stable chelators like $[^{111}In(DOTA)]^-$ and $[In(octapa)]^-$, it is still fair when compared to the very unstable ^{111}In-citrate complex, which has shown values of 18.7 ± 3.7% ID/g in the kidneys after 24 h.[57]

Often $^{111}InCl_3$ and ^{111}In-citrate are used to emulate the conditions of an unstable chelator that would undergo complete and rapid decomposition/transchelation in vivo. One commonly cited study (Ando et al.) has shown $^{111}InCl_3$ to have higher liver, spleen, and kidney uptake than ^{111}In-citrate;[56] however, another study has shown the kidney uptake of $^{111}InCl_3$ at 24 h in healthy rats to be 2.58 ± 0.83% ID/g,[58] which is significantly less than the value for ^{111}In-citrate cited above of 18.7 ± 3.7% ID/g,[57] and contradicts the observations from Ando et al.[56] Additionally, the highly anionic ^{111}In-citrate clears much more quickly through the kidneys than $^{111}InCl_3$, demonstrating that the hypothesis of rapid and complete dissociation upon introduction of these radiometal species into an animal is not accurate.[56] Considering these inconsistencies, it is important to utilize internal standards (such as $[^{111}In(DOTA)]^-$ in this study), and additionally there is a need for more clear and reliable baseline data for the biodistribution of ^{111}In in its most commonly used forms.[56,59,60]

dx.doi.org/10.1021/ja3024725 | J. Am. Chem. Soc. 2012, 134, 8670−8683

In biological systems, transchelated indium is nearly all bound to transferrin, with a maximum stability constant of log K_{ML} = 18.3.[55] Demetalation and hydroxide formation is a significant concern for acidic metal ions like Ga^{3+} and In^{3+}, and a conditional stability constant for transferrin that takes hydrolysis into account has been calculated as being ~10.0 for In^{3+}, which is higher even than Ga^{3+} at 6.9 and close to Fe^{3+} at 11.4.[55] This demonstrates the strong competition that transferrin holds for In^{3+} in vivo; however, the ligand exchange kinetics of In^{3+} are quite slow and it forms a more inert complex with transferrin than do Ga^{3+} and Fe^{3+}.[55,61] It is most likely that, due to the high stability and inertness of complexes like $[In(DOTA)]^-$ and the slow exchange kinetics with transferrin, only gradual in vivo decomplexation is observed over long periods such as >24 h. The higher levels of ^{111}In in the kidneys, liver, and spleen observed for $[In(DOTA)]^-$ after 24 h is most likely a result of this gradual exchange process, and the improved inertness and clearance observed for $[^{111}In(octapa)]^-$ correlates well with its lower isomerization and higher pM value of 26.8(1) ($[In(DOTA)]^-$ pM = 18.8) (Table 1) and suggests superior kinetic inertness. Additionally, the lower levels of ^{111}In in the kidneys at 24 h seen for $[In(octapa)]^-$, being roughly a third of that of $[In(DOTA)]^-$, are very promising because persistent kidney uptake is observed with many peptide conjugates of DOTA, CHX-A″-DTPA, and especially DTPA.[2,20,21,28−30,48] High residual activity in the kidneys can decrease image quality and obstruct delineation of tumors, decrease the accuracy of dosimetry, and deliver harmful doses of radiation to the healthy and nontargeted kidneys when used with therapeutic isotopes such as ^{90}Y.

CONCLUSIONS

Preliminary investigations of the octadentate acyclic chelator H_4octapa (N_4O_4) with $^{111}In/In^{3+}$ have demonstrated it to be a significant improvement on the shortcomings of the current industry gold standards, DOTA (N_4O_4) and DTPA (N_3O_5). Four major points were identified in the discussion as guidelines to be used in selecting an ideal chelating agent for radiometal ions, and $[In(octapa)]^-$ has been shown to be superior to $[In(DOTA)]^-$ and $[In(DTPA)]^{2-}$ for a majority of these points. We have demonstrated the ability of H_4octapa to quantitatively radiolabel ^{111}In at ambient temperature, which, in contrast to DOTA, allows it to be effectively used with sensitive biovectors like antibodies. H_4octapa has been radiolabeled with ^{111}In in 10 min at ambient temperature with specific activities as high as 2.3 mCi/nmol (97.5% radiochemical yield). In vitro mouse serum stability assays have demonstrated H_4octapa to have slightly improved stability with ^{111}In compared to that of DOTA and DTPA over 24 h, within error. Mouse biodistribution studies have shown that the radiometal complex $[^{111}In(octapa)]^-$ has exceptionally high in vivo stability and kinetic inertness, and compared to those of $[^{111}In(DOTA)]^-$, $[^{111}In(octapa)]^-$ has improved stability and improved clearance from the kidneys, liver, and spleen at 24 h. $^1H/^{13}C$ NMR studies of the $[In(octapa)]^-$ complex have revealed a 7-coordinate solution structure, which forms a single isomer and exhibits no observable fluxional behavior at ambient temperature on the NMR time scale and is an improvement on the isomerization observed with $[In(DTPA)]^{2-}$ and the fluxional isomerization of $[In(DOTA)]^-$.[40−42] Potentiometric titrations have determined the thermodynamic formation constant of the $[In(octapa)]^-$ complex to be log K_{ML} = 26.8(1) (pM = 26.5), which reveals a higher pM value than those determined for $[In(DOTA)]^-$ and $[In(DTPA)]^{2-}$ (18.8 and 25.7, respectively). The same set of experiments and analyses was performed with the potentially decadentate chelator H_5decapa (N_5O_5) and its $[In(decapa)]^{2-}$ complex; however, the formation of multiple isomers observed via HPLC radiotraces and NMR studies was not optimal, and unfavorable organ uptake and clearance were observed in biodistribution studies performed in mice. These results for H_5decapa suggest that it is not a suitable candidate for ^{111}In radiopharmaceutical elaboration; however, it may be a suitable candidate for coordinating lanthanide and actinide radiometal ions that can accommodate higher denticities, such as ^{90}Y, ^{177}Lu, and ^{225}Ac. The relatively simple five-step synthesis of H_4octapa is achieved with a cumulative yield of ~12%, and the five-step synthesis of H_5decapa was completed with a cumulative yield of ~2.5%. Optimization of reaction conditions and/or exploration of alternative protecting groups may improve these yields. Our initial investigations have revealed the acyclic chelator H_4octapa to be a valuable alternative to the macrocycle DOTA and the acyclic chelator DTPA by showing improved stability and kinetic inertness, as well as fast ambient temperature radiolabeling kinetics. Pending the results of investigations with ^{90}Y and ^{177}Lu, H_4octapa could present a very strong alternative to DOTA as an ideal chelator for incorporation into radiometal-based radiopharmaceuticals.

EXPERIMENTAL SECTION

Materials and Methods. All solvents and reagents were purchased from commercial suppliers (TCI America, Sigma Aldrich, Fisher Scientific) and were used as received. Mouse serum was purchased frozen from Sigma Aldrich. DOTA was purchased from Macrocyclics. The acyclic chelator H_2dedpa was synthesized according to the literature.[33,36] The analytical thin-layer chromatography (TLC) plates used were aluminum-backed ultrapure silica gel 60 Å, 250 μm thickness; the flash column silica gel (standard grade, 60 Å, 32−63 mm) was provided by Silicycle. ^1H and ^{13}C NMR spectra were recorded at ambient temperature on Bruker AV300, AV400, or AV600 instruments; the NMR spectra are expressed on the δ scale and were referenced to residual solvent peaks and/or internal tetramethylsilane. ^{13}C NMR experiments run in D_2O were externally referenced to a sample of CH_3OD/D_2O. Low-resolution mass spectrometry was performed using a Waters ZG spectrometer with an ESCI electrospray/chemical-ionization source, and high-resolution electrospray-ionization mass spectrometry (ESI-MS) was performed on a Micromass LCT time-of-flight instrument at the Department of Chemistry, University of British Columbia. Microanalysis for C, H, and N was performed on a Carlo Erba Elemental Analyzer EA 1108. IR spectra were collected neat in the solid state on a Thermo Nicolet 6700 FT-IR spectrometer. ^{111}In(chelate) mouse serum stability experiments were analyzed using GE Healthcare Life Sciences PD-10 desalting columns (size exclusion for MW < 5000 Da) and counted with a Capintec CRC 15R well counter. Radiolabeling of DOTA with ^{111}In was performed using a Biotage Initiator microwave reactor (μW). The HPLC system used for analysis and purification of cold compounds consisted of a Waters 600 controller, Waters 2487 dual wavelength absorbance detector, and a Waters delta 600 pump. Phenomenex synergi hydro-RP 80 Å columns (250 mm × 4.6 mm analytical and 250 mm × 21.2 mm semipreparative) were used for purification of several of the deprotected chelators. Analysis of radiolabeled complexes was carried out using a Waters xbridge BEH130 C18 reverse phase (150 mm × 6 mm) analytical column using a Waters Alliance HT 2795 separation module equipped with a Raytest Gabi Star NaI (Tl) detector and a Waters 996 photodiode array (PDA) detector. $^{111}InCl_3$ was cyclotron produced and provided by Nordion as a ~0.05 M HCl solution.

dx.doi.org/10.1021/ja3024725 | J. Am. Chem. Soc. 2012, 134, 8670−8683

Methyl 6-(Hydroxymethyl)picolinate (1). **1** was synthesized according to a modified literature protocol.[62] To a suspension of dimethylpyridine-2,6-dicarboxylate (10.0 g, 51.2 mmol) in methanol (400 mL), cooled in a salted ice bath, was slowly added sodium borohydride (5.56 g, 146.9 mmol, 2.4 equiv) over a period of 1 h, where the reaction mixture turned pink upon the addition of sodium borohydride. The reaction mixture was stirred and kept on ice for 4 h. After 4 h, TLC analysis revealed that the reaction mixture contained starting material (R_f: 0.45, TLC in 100% EtOAc), product (R_f: 0.33), and doubly reduced product (R_f: 0.24). The reaction mixture was quenched regardless of the remaining starting material in order to prevent over-reduction. The solution was diluted using dichloromethane (200 mL) and then quenched using saturated $NaHCO_3$ (~200 mL). The aqueous and organic layers were separated, and much of the methanol from the aqueous phase was evaporated in vacuo. The aqueous layer was then extracted with chloroform (2 × 100 mL) and ethyl acetate (3 × 100 mL). The combined organic layers were dried ($MgSO_4$), filtered, and concentrated in vacuo to dryness. The resulting white solid was purified by column chromatography (column 10" L × 2" W, eluted with a gradient of 3:1 ethyl acetate/petroleum ether to 100% ethyl acetate) to afford the product as a white solid (4.35 g, 51%, R_f: 0.33 in 100% EtOAc). ^{1}H NMR (300 MHz, $CDCl_3$): δ = 7.95 (d, 1H, pyr-*H*), 7.79 (t, 1H, pyr-*H*), 7.55 (d, 1H, pyr-*H*), 4.83 (s, 2H, methylene-*H*), 4.31 (s, 1H, -O*H*), 3.92 (s, 3H, methyl-*H*). ^{13}C NMR (75 MHz, $CDCl_3$): δ 165.44, 160.62, 146.69, 137.57, 123.95, 123.54, 64.57, 52.72. HR-ESI-MS calcd for $[C_8H_9NO_3 + H]^+$: 168.0661; found $[M + H]^+$ 168.0658.

Methyl 6-(Bromomethyl)picolinate (2). **2** was synthesized according to a modified literature protocol.[62] To a solution of **1** (4.00 g, 23.9 mmol) in chloroform (100 mL) under argon at 0 °C was added phosphorus tribromide (2.50 mL, 26.3 mmol, 1.1 equiv) in chloroform (10 mL) dropwise over 15 min via dropping funnel. A white precipitate formed, and then the solution turned bright yellow. The dropping funnel was rinsed using chloroform (15 mL), and the reaction mixture was stirred at 0 °C and monitored by TLC. A miniworkup using sodium carbonate in water and ethyl acetate was required to see reaction progress by TLC. At 3.5 h TLC indicated the quantitative conversion of alcohol to alkyl halide. The reaction mixture was quenched using sodium carbonate in water (75 mL) and was extracted with chloroform (4 × 25 mL). The combined organic layers were dried over $MgSO_4$, filtered, and concentrated in vacuo to dryness to afford an off-white solid. The crude product was purified through a short silica plug (2" L × 2" W, 25% EtOAc in petroleum ether) to afford **2** as an off-white solid (5.55 g, >99%, R_f: 0.64 in 30% petroleum ether in EtOAc). ^{1}H NMR (400 MHz, $CDCl_3$): δ 8.01 (d, 1H, pyr-*H*), 7.84 (t, 1H, pyr-*H*), 7.65 (d, 1H, pyr-*H*), 4.61 (s, 2H, methylene-*H*), 3.96 (s, 3H, methyl-*H*). ^{13}C NMR (100 MHz, $CDCl_3$): δ 165.07, 157.22, 147.36, 138.16, 127.03, 124.31, 53.93, 32.91. HR-ESI-MS calcd for $[C_8H_8NO_2{}^{79}Br + H]^+$: 229.9817; found $[M + H]^+$: 229.9812.

***N,N′*-(Benzyl)ethylenediamine (3).** To a solution of ethylenediamine (2.78 mL, 41.6 mmol) in dry methanol (distilled over CaH_2, 100 mL) was added benzaldehyde (8.48 mL, 83.2 mmol, 2 equiv). The solution was refluxed for 4 h and then cooled via an ice bath. Addition of $NaBH_4$ (6.77 g, 179 mmol, 4.3 equiv) was performed slowly and in small portions to prevent boiling, and the reaction mixture was stirred for 4 h until completion. The solvent was evaporated in vacuo, and then saturated $NaHCO_3$ (~50 mL), water (~50 mL) and chloroform (200 mL) were added. The aqueous layer was extracted twice more with chloroform (100 mL). The combined organic layers were dried over $MgSO_4$, filtered, and concentrated in vacuo to afford a waxy, yellow solid. Product was purified by silica column chromatography (column 10" L × 2" W, eluted with a gradient of 100% dichloromethane to 25% CH_3OH in dichloromethane) to afford **3** as yellow oil (4.90 g, 49%, R_f: 0.33 in 20% CH_3OH in dichloromethane). ^{1}H NMR (400 MHz, $CDCl_3$): δ 7.42 (d, 8H, Bn-*H*), 7.34 (m, 2H, Bn-*H*), 3.86 (s, 4H, Bn-CH_2–N), 2.83 (s, 4H, ethylene-*H*), 1.72 (s, 2H, amine-*H*). ^{13}C NMR (100 MHz, $CDCl_3$): δ 140.17, 127.94, 127.70, 126.45, 53.50, 48.39. HR-ESI-MS calcd for $[C_{16}H_{20}N_2 + H]^+$: 241.1705; found $[M + H]^+$: 241.1703.

***N,N′*-(Benzyl)-*N,N′*-[(*tert*-butoxycarbonyl)methyl]-ethylenediamine (4).** To a solution of **3** (1.0 g, 4.2 mmol) and sodium carbonate (1.76 g, 16.6 mmol, 3.9 equiv) in dry acetonitrile (distilled over CaH_2, 80 mL) was added dropwise a solution of *tert*-butyl bromoacetate (1.31 mL, 8.88 mmol, 2.1 equiv). The reaction mixture was stirred at 60 °C for 16 h. TLC (5% CH_3OH in dichloromethane) showed quantitative conversion of **3** to the tertiary diamine. Sodium carbonate was filtered and the filtrate concentrated in vacuo to dryness. The resulting yellow oil was purified by column chromatography (column 2" L × 2" W, eluted with a gradient of 100% petroleum ether to 10% ethyl acetate in petroleum ether) to afford **4** as a yellow solid (1.85 g, 93%, R_f: 0.59 in 5% CH_3OH in dichloromethane). ^{1}H NMR (400 MHz, $CDCl_3$): δ 7.40–7.29 (m, 10H, Bn-*H*), 3.85 (s, 4H, Bn-CH_2–N), 3.30 (s, 4H, $(CH_3)_3CO$–C(O)–CH_2–N), 2.88 (s, 4H, ethylene-*H*), 1.52 (s, 18H, $(CH_3)_3CO$–C(O)–CH_2–N). ^{13}C NMR (100 MHz, $CDCl_3$): δ 170.80, 139.13, 128.83, 128.08, 126.85, 80.51, 58.30, 55.06, 51.60, 28.11. HR-ESI-MS calcd for $[C_{28}H_{40}N_2O_4 + H]^+$: 469.3066; found $[M + H]^+$: 469.3055.

***N,N′*-[(*tert*-Butoxycarbonyl)methyl]ethylenediamine (5).** To a solution of **4** (776.3 mg, 1.656 mmol) in glacial acetic acid (7 mL) was added Pd/C (78 mg, ~10 wt %). Hydrogen gas was bubbled through the solution for 3 min, and then the reaction mixture was stirred under a hydrogen atmosphere (balloon) for 16 h. The Pd/C was filtered out over Celite, rinsing well with methanol, and the filtrate was evaporated to dryness in vacuo. The crude product was purified by silica gel column chromatography (eluted with a gradient of 100% dichloromethane to 5% methanol in dichloromethane) and identified by TLC using an I_2 chamber to stain. Product fractions were combined and concentrated in vacuo to afford the product **5** as a waxy yellow solid (0.51 g, 87%, R_f: 0.20 in 10% CH_3OH in dichloromethane). ^{1}H NMR (300 MHz, $CDCl_3$): δ 3.37 (s, 4H, $(CH_3)_3CO$–C(O)–CH_2–N), 2.68 (s, 4H, ethylene-*H*), 2.03 (s, 2H, –N*H*–), and 1.43 (s, 18H, $(CH_3)_3CO$–C(O)–CH_2–N). ^{13}C NMR (75 MHz, $CDCl_3$): δ 171.67, 80.96, 51.46, 48.76, 28.01. HR-ESI-MS calcd for $[C_{14}H_{28}N_2O_4 + H]^+$: 289.2127; found $[M + H]^+$: 289.2126.

***N,N′*-[(*tert*-Butoxycarbonyl)methyl]-*N,N′*-{[6-(methoxycarbonyl)pyridin-2-yl]methyl}ethylenediamine (6).** To a solution of **5** (431.5 mg, 1.496 mmol) and **2** (725 mg, 3.142 mmol, 2.1 equiv) in dry acetonitrile (distilled over CaH_2, 20 mL) was added sodium carbonate (~300 mg). The solution was heated for 16 h at 60 °C under argon. Sodium carbonate was removed by filtration and rinsed with acetonitrile. The filtrate was concentrated in vacuo to dryness, and the resulting yellow oil was purified by column chromatography (eluted with a gradient of 100% dichloromethane to 5% methanol in dichloromethane) to afford **6** as colorless oil (342 mg, 39%, R_f: 0.40 in 10% CH_3OH in dichloromethane). ^{1}H NMR (300 MHz, $CDCl_3$): δ 7.85–7.82 (m, 2H, pyr-H), 7.65–7.63 (m, 4H, pyr-H), 3.85 (s, 4H, Pyr-CH_2–), 3.83 (s, 6H, –O–CH_3), 3.16 (s, 4H, $(CH_3)_3CO$–CO–CH_2–N), 2.67 (s, 4H, ethylene-H), 1.28 (s, 18H, $(CH_3)_3CO$–C(O)–CH_2–N). ^{13}C NMR (75 MHz, $CDCl_3$): δ 170.16, 165.39, 160.34, 146.74, 137.13, 125.84, 123.19, 80.66, 60.17, 55.98, 52.44, 52.09, 27.73. HR-ESI-MS calcd for $[C_{30}H_{42}N_4O_8 + H]^+$: 587.3081; found $[M + H]^+$: 587.3091.

H_4octapa·4HCl·2H_2O. *N,N′*-Bis(6-carboxy-2-pyridylmethyl)-ethylenediamine-*N,N′*-diacetic Acid. A portion of **6** (277.4 mg, 0.4728 mmol) was dissolved in HCl (6 M) and refluxed for 8 h. White solid was observed to precipitate from hot HCl (aq) below ~60 °C. The solution was then cooled in the freezer for 1 h. The product was filtered and washed with cold ethanol and diethyl ether to afford the HCl salt **H_4octapa** as a white solid (265 mg, 75% yield using the molecular weight of the HCl salt from elemental analysis). ^{1}H NMR (300 MHz, D_2O): δ 8.12–8.02 (m, 4H, pyr-*H*), 7.72–7.69 (d, 2H, pyr-*H*), 4.53 (s, 4H, Pyr-CH_2–N), 3.97 (s, 4H, HOOC–CH_2–N), 3.57 (s, 4H, ethylene-*H*). ^{13}C NMR (75 MHz, D_2O): δ 170.65, 165.57, 151.46, 145.43, 142.90, 128.83, 126.36, 58.07, 55.22, 51.48. IR (neat, ATR-IR): ν = 1720.9 cm^{-1} (C═O), 1635.9/1618.2 cm^{-1} (C═C py). HR-ESI-MS calcd for $[C_{20}H_{20}N_4O_8 + H]^+$: 445.1359; found $[M + H]^+$: 445.1368. Elemental analysis: calcd % for H_4octapa·4HCl·2H_2O ($C_{20}H_{20}N_4O_8$·4HCl·2H_2O = 628.283): C 38.23, H 4.81, N 8.92; found: C 38.34, H 4.81, N 8.93.

dx.doi.org/10.1021/ja3024725 | *J. Am. Chem. Soc.* 2012, 134, 8670–8683

Na[In(octapa)]. Portions of H_4octapa·4HCl·$2H_2O$ (9.9 mg, 0.019 mmol) and $In(ClO_4)_3·8H_2O$ (11.7 mg, 0.021 mmol, 1.1 equiv) were dissolved in HCl (aq) (1 mL, 0.1 M) in a 1 dram screw-cap vial. The pH was adjusted to ∼4.5 with NaOH (aq) (0.1 M) while stirring. The reaction mixture was stirred at 60 °C for 4 h, then evaporated to dryness to afford Na[In(octapa)] as a white solid. ^{1}H NMR (600 MHz, D_2O): δ 8.34−8.32 (m, 2H, pyr-*H*), 8.23 (d, 2H, pyr-*H*), 7.85 (d, 2H, Pyr-*H*), 4.49 (d, 2H, Pyr-CH_2−N, ^2J = 16.1 Hz), 4.34 (d, 2H, Pyr-CH_2−N, ^2J = 16.1 Hz), 3.27 (d, 2H, HOOC−CH_2−N, ^2J = 19.3 Hz), 3.19−3.18 (broad d, 2H, HOOC−CH_2−N, ^2J = 8.4 Hz), 3.07−3.04 (m, 4H, ethylene-*H*). ^{13}C NMR (150 MHz, D_2O): δ 177.25, 167.84, 153.68, 148.21, 144.21, 128.27, 124.57, 59.39, 58.35, 55.24. HR-ESI-MS calcd for $[C_{20}H_{18}{}^{115}InN_4O_8 + 2·Na]^+$: 602.9959; found $[M + 2·Na]^+$: 602.9942.

***N,N″*-(Benzyl)diethylenetriamine (7).** To a solution of diethylenetriamine (5 mL, 46.2 mmol) in dry methanol (distilled over CaH_2, 100 mL) was added benzaldehyde (9.43 mL, 96.56 mmol, 2 equiv). The solution was refluxed for 4 h, and then cooled (0 °C) via ice bath. Addition of $NaBH_4$ (12.26 g, 323 mmol, 7 equiv) was performed slowly and in small portions to prevent boiling. The reaction solution was stirred for 4 h until completion. The solvent was evaporated in vacuo, and then saturated $NaHCO_3$ (∼100 mL) and chloroform (200 mL) were added. The aqueous layer was extracted twice more with dichloromethane (100 mL). The combined organic layers were dried over $MgSO_4$, filtered, and concentrated in vacuo to afford a yellow solid. The crude product was purified by silica gel column chromatography (column 16" L × 3" W, eluted with a gradient of 2 to 10% CH_3OH and 2% triethylamine in dichloromethane) to afford **7** as yellow oil (5.23 g, 40%, R_f: 0.30 in 20% CH_3OH in dichloromethane). ^{1}H NMR (300 MHz, $CDCl_3$): δ 7.34−7.26 (m, 10H, Bn-*H*), 3.80 (s, 4H, Bn-CH_2−N), 2.75 (s, 8H, ethylene-*H*), 1.94 (s, 3H, −N*H*−). ^{13}C NMR (75 MHz, $CDCl_3$): δ 140.54, 128.64, 128.34, 127.11, 54.08, 49.39, 48.92. HR-ESI-MS calcd for $[C_{18}H_{25}N_3 + H]^+$: 284.2127; found $[M + H]^+$: 284.2124.

***N,N″*-(Benzyl)-*N,N′,N″*-[(*tert*-butoxycarbonyl)methyl]-diethylenetriamine (8).** To a solution of **7** (673.3 mg, 2.37 mmol) and sodium carbonate (excess, 450 mg) in dry acetonitrile (distilled over CaH_2, 20 mL) was added dropwise *tert*-butyl bromoacetate (1.071 mL, 7.25 mmol, 3.05 equiv) under argon. The solution was stirred at 60 °C for 20 h. Sodium carbonate was filtered and the filtrate concentrated in vacuo to dryness. The resulting yellow oil was purified by column chromatography (column 10" L × 2" W, eluted with a gradient of 1 CH_3OH to 10% CH_3OH in dichloromethane) to afford **8** as light-yellow oil (974.4 mg, 66%, R_f: 0.36 in 10% CH_3OH in dichloromethane). ^{1}H NMR (400 MHz, $CDCl_3$): δ 7.41−7.29 (m, 10H, Bn-*H*), 3.86 (s, 4H, Bn-CH_2−N), 3.39 (s, 2H, $(CH_3)_3$CO−CO−CH_2−N′), 3.31 (s, 4H, $(CH_3)_3$CO−CO−CH_2−N/N″), 2.84 (s, 8H, ethylene-*H*), 1.54 (s, 18H, $(CH_3)_3$CO−CO−CH$_2$−N/N″), 1.50 (s, 9H, $(CH_3)_3$CO−CO−CH$_2$−N′). ^{13}C NMR (100 MHz, $CDCl_3$): δ 170.86, 170.69, 139.06, 128.79, 128.03, 126,82, 80.45, 80.39, 58.24, 55.88, 55.05, 52.45, 51.89, 28.08, 28.03. HR-ESI-MS calcd for $[C_{36}H_{55}N_3O_6 + H]^+$: 626.4169; found $[M + H]^+$: 626.4166.

***N,N′,N″*-[(*tert*-Butoxycarbonyl)methyl]diethylenetriamine (9).** To a solution of **8** (702.6 mg, 1.12 mmol) in glacial acetic acid (10 mL) was added Pd/C (35 mg, ∼5 wt %). Hydrogen gas was bubbled through the solution for 3 min, and then the reaction mixture was stirred under a hydrogen atmosphere (balloon) for 16 h. The Pd/C was filtered over Celite, rinsing with methanol, and then the filtrate was evaporated to dryness in vacuo. The crude product was purified by silica gel column chromatography (0 to 10% methanol in dichloromethane) and identified by TLC using an I_2/silica chamber to stain. Product fractions were combined and concentrated in vacuo to dryness to afford the product **9** as colorless oil (150 mg, 30%, R_f: 0.26 in 2.5% CH_3OH and 2.5% triethylamine in dichloromethane). Cleavage of the ethylene bridges was observed during hydrogenation and produced large amounts of byproduct. ^{1}H NMR (300 MHz, $CDCl_3$): δ 3.28 (s, 2H, $(CH_3)_3$CO−CO−CH_2−N′), 3.25 (s, 4H, $(CH_3)_3$CO−CO−CH_2−N/N″), 2.77−2.73 (m, 4H, ethylene-*H*), 2.62−2.59 (m, 4H, ethylene-*H*), 2.14 (s, 2H, −N*H*−), 1.40 (s, 18H, $(CH_3)_3$CO−CO−CH$_2$−N/N″), 1.39 (s, 9H, $(CH_3)_3$CO−CO−CH$_2$−N′). ^{13}C NMR (75 MHz, $CDCl_3$): δ 170.45, 170.78, 80.76, 80.67, 55.56, 54.03, 51.51, 47.17, 28.05, 27.98. HR-ESI-MS calcd for $[C_{22}H_{43}N_3O_6 + H]^+$: 446.3230; found $[M + H]^+$: 446.3239.

***N,N″*-{[6-(Methoxycarbonyl)pyridin-2-yl]methyl}-*N,N′,N″*-[(*tert*-butoxycarbonyl)methyl]diethylenetriamine (10).** To a solution of **9** (101.8 mg, 0.228 mmol) and **2** (110.4 mg, 0.479 mmol, 2.1 equiv) in dry acetonitrile (distilled over CaH_2, 10 mL) was added sodium carbonate (∼100 mg). The solution was heated for 16 h at 60 °C under argon. Sodium carbonate was removed by filtration and rinsed with acetonitrile. The filtrate was concentrated in vacuo to dryness, and the resulting yellow oil was purified by column chromatography (100% dichloromethane to 5% CH_3OH in dichloromethane) to afford **10** as colorless oil (75.7 mg, 45%, R_f: 0.27 in 2.5% CH_3OH and 2.5% triethylamine in dichloromethane). ^{1}H NMR (300 MHz, $CDCl_3$): δ 7.96−7.94 (m, 2H, Pyr-*H*), 7.82−7.70 (m, 4H, Pyr-*H*), 3.97 (s, 4H, Pyr-CH_2−N), 3.96 (s, 6H, −O−CH_3), 3.28 (s, 4H, $(CH_3)_3$CO−CO−CH_2−N/N″), 3.23 (s, 2H, $(CH_3)_3$CO−CO−CH_2−N′), 2.72 (s, 8H, ethylene-*H*), 1.41 (s, 18H, $(CH_3)_3$CO−CO−CH$_2$−N/N″), 1.37 (s, 9H, $(CH_3)_3$CO−CO−CH$_2$−N′). ^{13}C NMR (75 MHz, $CDCl_3$): δ 170.66, 170.45, 170.37, 165.80, 160.93, 147.06, 137.29, 126.01, 123.45, 80.91, 80.85, 80.64, 60.52, 56.36, 56.29, 55.77, 52.74, 56.68, 55.77, 52.74, 52.68, 52.62, 52.42, 28.07. HR-ESI-MS calcd for $[C_{38}H_{57}N_5O_{10} + H]^+$: 744.4184; found $[M + H]^+$: 744.4199.

H_5decapa·5HCl·2.5H_2O. *N,N″*-{[6-(Carboxy)pyridin-2-yl]-methyl}diethylenetriamine-*N,N′,N″*-triacetic Acid. A portion of **10** (76.7 mg, 0.1031 mmol) was dissolved in HCl (6 M) and refluxed for 8 h. The reaction mixture was concentrated in vacuo to an off-white powder, which was then purified by reverse-phase HPLC (gradient: A: 0.1% TFA (trifluoroacetic acid), B: CH_3CN; 0 to 100% B linear gradient 25 min. t_R = broad, 13.2−15 min). The HPLC fractions were combined, 2 mL of HCl (6 M) was added, and the solvent was removed in vacuo to drive off residual trifluoroacetic acid. Another 2 mL of HCl (6 M) was added and then concentrated in vacuo to afford the HCl salt of H_5decapa as a white solid (56 mg, 71% using molecular weight from elemental analysis). ^{1}H NMR (400 MHz, D_2O): δ 8.11−8.04 (m, 4H, Pyr-*H*), 7.72−7.71 (m, 2H, Pyr-*H*), 4.55 (s, 4H, Pyr-CH_2−N), 3.98 (s, 4H, HOOC−CH_2−N/N″), 3.71 (s, 2H, HOOC−CH_2−N′), 3.44 (s, 4H, ethylene-*H*), 3.28 (s, 4H, ethylene-*H*). ^{13}C NMR (100 MHz, D_2O): δ 172.54, 170.22, 168.18, 151.08, 145.92, 142.33, 128.81, 126.33, 57.89, 54.96, 54.27, 51.99, 50.82. IR (neat, ATR-IR): ν = 1727.2 cm^{-1} (C═O), 1642.7 cm^{-1} (C═C py). HR-ESI-MS calcd for $[C_{24}H_{29}N_5O_{10} + H]^+$: 548.1993; found $[M + H]^+$: 548.1987. Elemental analysis: calcd % for H_5decapa·5HCl·2.5H_2O ($C_{24}H_{29}N_5O_{10}$·5HCl·2.5H_2O = 774.856): C 37.20, H 5.07, N 9.04; found: C 37.28, H 4.91, N 8.72.

Na_2[In(decapa)]. A portion of H_5decapa (8.6 mg, 0.0112 mmol) and $In(ClO_4)_3·8H_2O$ (6.9 mg, 0.0124 mmol, 1.1 equiv) was dissolved in HCl (aq) (1 mL, 0.1 M) in a 1 dram screw-cap vial. The pH was adjusted to ∼4.5 with NaOH (aq) (0.1 M) while stirring. The reaction mixture was stirred at 60 °C for 16 h and then evaporated to dryness to afford Na_2[In(decapa)]. ^{1}H NMR (600 MHz, D_2O): δ 8.33−7.71 (m, 6H, Pyr-*H*), 4.87−2.57 (m, 18H, complex diastereotopic splitting). ^{13}C NMR (150 MHz, D_2O): δ 178.51, 178.35, 178.04, 177.42, 176.63, 168.43, 167.83, 154.01, 153.63, 148.54, 146.64, 145.44, 145.02, 144.17, 143.22, 142.83, 142.56, 128.77, 128.26, 128.12, 128.01, 124.42, 123.61, 123.53, 123.07, 61.29, 59.50, 59.31, 59.06, 58.32, 57.82, 55.71, 55.29, 53.99, 52.55, 52.46, 51.02. HR-ESI-MS calcd for $[C_{24}H_{24}{}^{115}InN_5O_{10} + H + 2Na]^+$: 704.0436; found $[M + H + 2Na]^+$: 704.0430.

H_2dedpa. The hexadentate chelator H_2dedpa was synthesized according to the literature,[33,35,36] with a modified purification step performed by reverse-phase HPLC (gradient: A: 0.1% TFA, B: CH_3CN; 0 to 100% B linear gradient 25 min. t_R = broad, 9.7−11 min), followed by a second HPLC purification with a modified gradient (A: distilled deionized water, B: CH_3CN; 0 to 100% B linear gradient 25 min. t_R = broad, 8.5−10 min).

[In(dedpa)]Cl. A portion of H_2dedpa (10 mg, 0.020 mmol) and $In(ClO_4)_3·8H_2O$ (13 mg, 0.023 mmol, 1.2 equiv) were dissolved in HCl (aq) (1 mL, 0.1 M) in a 1 dram screw-cap vial. The pH was adjusted to ∼4−4.5 with NaOH (aq) (0.1 M) while stirring. The

dx.doi.org/10.1021/ja3024725 | J. Am. Chem. Soc. 2012, 134, 8670−8683

reaction solution was stirred at 60 °C for 16 h, then evaporated to dryness to afford [In(dedpa)]Cl as a white solid. ^{1}H NMR (600 MHz, DMSO-d_6): δ 8.19 (t, 2H, pyr-*H*), 8.07 (d, 2H, pyr-*H*), 7.71 (d, 2H, pyr-*H*), 4.40 (s, 2H, −N*H*−), 4.27/4.26 (two overlapping d, 2H, Pyr-CH_2−N, ^2J = 16.6/16.3 Hz), 3.90/3.89 (two overlapping d, 2H, Pyr-CH_2−N, ^2J = 16.6 Hz), 2.63−2.56 (m, 4H, ethylene-*H*). ^{1}H NMR (400 MHz, D_2O): δ 8.28 (t, 2H, pyr-*H*), 8.20 (d, 2H, pyr-*H*), 7.79 (d, 2H, pyr-*H*), 4.58 (d, 2H, Pyr-CH_2−N, ^2J = 17.3 Hz), 4.13 (d, 2H, Pyr-CH_2−N, ^2J = 17.4 Hz), 2.96−2.81 (m, 4H, ethylene-*H*). ^{13}C NMR (300 MHz, DMSO-d_6): δ 163.74, 151.99, 146.94, 141.34, 124.62, 121.82, 49.48, 44.92. HR-ESI-MS calcd for $[C_{16}H_{16}{}^{115}InN_4O_4]^+$: 443.0210; found $[M]^+$: 443.0216.

^{111}In Radiolabeling Studies. The chelators H_4octapa, H_5decapa, H_2dedpa, DTPA, and DOTA were made up as stock solutions (1 mg/mL, ∼10^{-3} M) in deionized water. An aliquot of each chelator stock solution was transferred to screw-cap mass spectrometry vials and made up to 1 mL with pH 5.5 NaOAc (10 mM) buffer, to a final chelator concentration of ∼365 μM for each sample. A ∼10 μL aliquot of the $^{111}InCl_3$ stock solution (∼1 mCi for labeling studies and ∼5−7 mCi for mouse serum competitions) was transferred into the vials containing each chelator, allowed to radiolabel at ambient temperature for 10 min, and then analyzed by RP-HPLC to confirm radiolabeling and calculate yields. $[^{111}In(DOTA)]^-$ was heated at 80 °C for 20 min in a microwave reactor to achieve quantitative radiolabeling yields. Areas under the peaks observed in the HPLC radiotrace were integrated to determine radiolabeling yields. The highest specific activity of 2.3 mCi/nmol obtained for H_4octapa was the result of labeling a 990 μL solution of 3.65×10^{-7} M chelate in NaOAc buffer (pH 5.3, 10 mM) with 10 μL of $^{111}In^{3+}$ in a 0.05 M HCl solution (1.02 mCi) for 10 min at ambient temperature in 97.5% radiolabeling yield. Elution conditions used for RP-HPLC analysis were gradient: A: 10 mM NaOAc buffer pH 4.5, B: CH_3CN; 0 to 100% B linear gradient 20 min. The radiometal complex $[^{111}In(dedpa)]^+$ used a modified HPLC gradient of A: 10 mM NaOAc buffer pH 4.5, B: CH_3CN; 0 to 5% B linear gradient 20 min. $[^{111}In(dedpa)]^+$ (t_R = 5.9 min), $[^{111}In(octapa)]^-$ (t_R = 4.7 min), $[^{111}In(decapa)]^{2-}$ (t_R = 5.4 min {5%}, 7.7 min {95%}), $[^{111}In(DTPA)]^{2-}$ (t_R = 6.5 min), and $[^{111}In(DOTA)]^-$ (t_R = 3.5 min) were all formed in >99% radiochemical yields. Overlayed HPLC radiotraces are shown in Figure S27, SI, and some original radiotraces are shown in Figures S19−S22, SI.

Solution Thermodynamics. The experimental procedures and details of the apparatus closely followed those of a previous study for H_2dedpa with Ga^{3+}.[33] As a result of the strength of the binding of the In^{3+} complex $[^{111}In(octapa)]^-$, the complex formation constant with this ligand could not be determined directly and the ligand−ligand competition method using the known competitor Na_2H_2EDTA was used. For H_5decapa, the ligand−ligand competition method was not required owing to the presence of a stable MHL species, and instead it was titrated directly with In^{3+}. Potentiometric titrations were performed using a Metrohm Titrando 809 equipped with a Ross combination pH electrode and a Metrohm Dosino 800. Data were collected in triplicate using *PC Control* (Version 6.0.91, Metrohm). The titration apparatus consisted of a water-jacketed glass vessel maintained at 25.0 (±0.1 °C, Julabo water bath). Prior to and during the course of the titration, a blanket of nitrogen, passed through 10% NaOH to exclude any CO_2, was maintained over the sample solution. Indium ion solutions were prepared by dilution of the appropriate atomic absorption standard (AAS) solution. The exact amount of acid present in the indium standard was determined by titration of an equimolar solution of In^{3+} and Na_2H_2EDTA. The amount of acid present was determined by Gran's method.[63] Calibration of the electrode was performed prior to each measurement by titrating a known amount of HCl with 0.1 M NaOH. Calibration data were analyzed by standard computer treatment provided within the program *MacCalib*[64] to obtain the calibration parameters E_0. Equilibration times for titrations were 10 min for pK_a titrations and 15 min for metal complex titrations. Ligand and metal concentrations were in the range of 0.75−1.0 mM for potentiometric titrations. The data were treated by the program *Hyperquad2008*.[65] The four successive proton dissociation constants corresponding to hydrolysis of $In^{3+}{}_{aq}$ ion and the indium-chloride stability constants included in the calculations were taken from Baes and Mesmer.[66] All values and errors represent the average of at least three independent experiments.

Molecular Modeling. Calculations were performed using the *Gaussian 09*[67] and *GaussView* packages. Molecular geometries and electron densities were obtained from density functional theory calculations, with the B3LYP functional employing the 6-31+G(d,p) basis set for first- and second-row elements, and the ECP basis set, LANL2DZ, was employed for indium.[68,69] Solvent (water) effects were described through a continuum approach by means of the IEF PCM as implemented in G09. The electrostatic potential was mapped onto the calculated electron density surface.

Mouse Serum Stability Data. The compounds $[^{111}In(octapa)]^-$, $[^{111}In(decapa)]^{2-}$, $[^{111}In(DOTA)]^-$, $[^{111}In(DTPA)]^{2-}$, and $[^{111}In(dedpa)]^+$ were prepared with the radiolabeling protocol as described above. Mouse serum was removed from the freezer and allowed to thaw at ambient temperature for 30 min. In triplicate for each ^{111}In complex listed above, solutions were made in sterile vials with 750 μL mouse serum, 500 μL of ^{111}In-complex (10 mM NaOAc buffer, pH 5.5), and 250 μL phosphate buffered saline (PBS) and were left to sit at ambient temperature. After 1 h, half of the mouse serum competition mixture (750 μL) was removed from each vial, diluted to a total volume of 2.5 mL with phosphate buffered saline, and then counted in a Capintec CRC 15R well counter to obtain a value for the total activity to be loaded on the PD-10 column. The 2.5 mL of diluted mouse serum competition mixture was then loaded onto a PD-10 column that had previously been conditioned via elution with 20 mL of PBS. The 2.5 mL of loading volume was allowed to elute into a ^{111}In waste container, and then the PD-10 column was eluted with 3.5 mL PBS and collected into another sterile vial. The eluent which contained ^{111}In bound/associated with serum proteins (size exclusion for MW < 5000 Da) was counted in a well counter and then compared to the total amount of activity that was loaded on the PD-10 column to obtain the percentage of ^{111}In that was bound to serum proteins and therefore no longer chelate-bound. The percent stability values shown in Table 2 represent the percentage of ^{111}In that was retained on the PD-10 column and therefore still chelate-bound.

Biodistribution Data. The protocol used in these animal studies was approved by the Institutional Animal Care Committee (IACC) of the University of British Columbia (Protocol # A10-0171) and was performed in accordance with the Canadian Council on Animal Care Guidelines. A total of 16 female ICR mice (20−25 g, 6−8 weeks) were used for the biodistribution study of each of the three radiometal complexes. $[^{111}In(octapa)]^-$, $[^{111}In(DOTA)]^-$, and $[^{111}In(decapa)]^{2-}$ were prepared as described above and then diluted in phosphate-buffered saline to a concentration of 100 μCi/mL. Each mouse was intravenously injected through the tail vein with ∼10 μCi (100 μL) of the ^{111}In complex and then sacrificed by CO_2 inhalation 15 min, 1 h, 4 h, or 24 h after injection (n = 4 at each time point). Blood (500−700 μL) was collected by cardiac puncture with a 25 G needle and placed into an appropriate microtainer tube for scintillation counting. Urine was collected from the bladder after sacrifice and counted. Tissues collected included spleen, kidney, intestine, liver, heart, lung, brain, muscle, and femur. Tissues were weighed and counted with a Capintec CRC 15R well counter, and the counts were decay corrected from the first 15 min time point and then converted to the percentage of injected dose (% ID) per gram of organ tissue (% ID/g).

■ ASSOCIATED CONTENT

Ⓢ Supporting Information

Data and figures from potentiometric titrations, mouse serum stability assays, mouse biodistribution studies, original HPLC radio-traces, and ^{1}H/^{13}C NMR spectra of several compounds and metal−chelate complexes. This material is available free of charge via the Internet at http://pubs.acs.org.

AUTHOR INFORMATION

Corresponding Author

adam@triumf.ca; orvig@chem.ubc.ca

Notes

The authors declare no competing financial interest.

ACKNOWLEDGMENTS

We acknowledge Nordion (Canada) and the Natural Sciences and Engineering Research Council (NSERC) of Canada for grant support and for a CGS-M/CGS-D fellowship (E.W.P.), and Dr. Dawn Waterhouse from the BC Cancer Agency for performing the biodistribution experiments. C.O. acknowledges the Canada Council for the Arts for a Killam Research Fellowship (2011-2013).

REFERENCES

(1) Holland, J. P.; Williamson, M. J.; Lewis, J. S. *Mol. Imaging* **2010**, *9*, 1−20.

(2) Pauwels, S.; Barone, R.; Walrand, S.; Borson-Chazot, F.; Valkema, R.; Kvols, L. K.; Krenning, E. P.; Jamar, F. *J. Nucl. Med.* **2005**, *46*, 92S−98S.

(3) Rösch, F.; Baum, R. P. *Dalton Trans.* **2011**, *40*, 6104−6111.

(4) Zeglis, B. M.; Mohindra, P.; Weissmann, G. I.; Divilov, V.; Hilderbrand, S. A.; Weissleder, R.; Lewis, J. S. *Bioconjugate Chem.* **2011**, *22*, 2048−2059.

(5) Lubberink, M.; Tolmachev, V.; Widström, C.; Bruskin, A.; Lundqvist, H.; Westlin, J.-E. *J. Nucl. Med.* **2002**, *43*, 1391−1397.

(6) Rösch, F.; Qaim, S. M.; Novgorodov, A. F.; Ying-Ming, T. *Appl. Radiat. Isot.* **1997**, *48*, 19−26.

(7) Zeglis, B. M.; Lewis, J. S. *Dalton Trans.* **2011**, *40*, 6168−6195.

(8) Sharkey, R. M.; Burton, J.; Goldenberg, D. M. *Expert Rev. Clin. Immunol.* **2005**, *1*, 47−62.

(9) Hohloch, K.; Zinzani, P. L.; Linkesch, W.; Jurczak, W.; Deptala, A.; Lorsbach, M.; Windemuth-Kiesselbach, C.; Wulf, G. G.; Truemper, L. H. *Bone Marrow Transplant.* **2010**, *46*, 901−903.

(10) Lamb, H.; Faulds, D. *Drugs Aging* **1998**, *12*, 293−304.

(11) Shi, W.; Johnston, C. F.; Buchanan, K. D.; Ferguson, W. R.; Laird, J. D.; Crothers, J. G.; McIlrath, E. M. *QJM* **1998**, *91*, 295−301.

(12) Cremonesi, M.; Ferrari, M.; Zoboli, S.; Chinol, M.; Stabin, M. G.; Orsi, F.; Maecke, H. R.; Jermann, E.; Robertson, C.; Fiorenza, M.; Tosi, G.; Paganelli, G. *Eur. J. Nucl. Med. Mol. Imaging* **1999**, *26*, 877−886.

(13) Thakur, M. L.; Segal, A. W.; Louis, L.; Welch, M. J.; Hopkins, J.; Peters, T. J. *J. Nucl. Med.* **1977**, *18*, 1022−1026.

(14) Nayak, T. K.; Garmestani, K.; Milenic, D. E.; Baidoo, K. E.; Brechbiel, M. W. *PLoS One* **2011**, *6*, e18198.

(15) Nayak, T. K.; Garmestani, K.; Baidoo, K. E.; Milenic, D. E.; Brechbiel, M. W. *Int. J. Cancer* **2010**, *128*, 920−926.

(16) Palm, S.; Enmon, R. M.; Matei, C.; Kolbert, K. S.; Xu, S.; Zanzonico, P. B.; Finn, R. L.; Koutcher, J. A.; Larson, S. M.; Sgouros, G. *J. Nucl. Med.* **2003**, *44*, 1148−1155.

(17) Gordon, L. I.; Witzig, T. E.; Wiseman, G. A.; Flinn, I. W.; Spies, S. S.; Silverman, D. H.; Emmanuolides, C.; Cripe, L.; Saleh, M.; Czuczman, M. S.; Olejnik, T.; White, C. A.; Grillo-López, A. J. *Semin. Oncol.* **2002**, *29*, 87−92.

(18) Giblin, M. F.; Veerendra, B.; Smith, C. J. *In Vivo* **2005**, *19*, 9−29.

(19) Herzog, H.; Rösch, F.; Stöcklin, G.; Lueders, C.; Qaim, S. M.; Feinendegen, L. E. *J. Nucl. Med.* **1993**, *34*, 2222−2226.

(20) Förster, G. J.; Engelbach, M. J.; Brockmann, J. J.; Reber, H. J.; Buchholz, H. G.; Mäcke, H. R.; Rösch, F. R.; Herzog, H. R.; Bartenstein, P. R. *Eur. J. Nucl. Med.* **2001**, *28*, 1743−1750.

(21) Carrasquillo, J. A.; White, J. D.; Paik, C. H.; Raubitschek, A.; Le, N.; Rotman, M.; Brechbiel, M. W.; Gansow, O. A.; Top, L. E.; Perentesis, P.; Reynolds, J. C.; Nelson, D. L.; Waldmann, T. A. *J. Nucl. Med.* **1999**, *40*, 268−276.

(22) Sprague, J. E.; Peng, Y.; Fiamengo, A. L.; Woodin, K. S.; Southwick, E. A.; Weisman, G. R.; Wong, E. H.; Golen, J. A.; Rheingold, A. L.; Anderson, C. J. *J. Med. Chem.* **2007**, *50*, 2527−2535.

(23) Garrison, J. C.; Rold, T. L.; Sieckman, G. L.; Figueroa, S. D.; Volkert, W. A.; Jurisson, S. S.; Hoffman, T. J. *J. Nucl. Med.* **2007**, *48*, 1327−1337.

(24) Nayak, T. K.; Garmestani, K.; Baidoo, K. E.; Milenic, D. E.; Brechbiel, M. W. *J. Nucl. Med.* **2010**, *51*, 942−950.

(25) Schneider, D. W.; Heitner, T.; Alicke, B.; Light, D. R.; McLean, K.; Satozawa, N.; Parry, G.; Yoo, J.; Lewis, J. S.; Parry, R. *J. Nucl. Med.* **2009**, *50*, 435−443.

(26) Rösch, F.; Herzog, H.; Stolz, B.; Brockmann, J.; Köhle, M.; Mühlensiepen, H.; Marbach, P.; Müller-Gärtner, H.-W. *Eur. J. Nucl. Med. Mol. Imaging* **1999**, *26*, 358−366.

(27) Boswell, C. A.; Brechbiel, M. W. *Nucl. Med. Biol.* **2007**, *34*, 757−778.

(28) Wu, C.; Kobayashi, H.; Sun, B.; Yoo, T. M.; Paik, C. H.; Gansow, O. A.; Carrasquillo, J. A.; Pastan, I.; Brechbiel, M. W. *Bioorg. Med. Chem.* **1997**, *5*, 1925−1934.

(29) Camera, L.; Kinuya, S.; Garmestani, K.; Wu, C.; Brechbiel, M. W.; Pai, L. H.; McMurry, T. J.; Gansow, O. A.; Pastan, I.; Paik, C. H.; Carrasquillo, J. A. *J. Nucl. Med.* **1994**, *35*, 882−889.

(30) Brechbiel, M. W.; Gansow, O. A.; Atcher, R. W.; Schlom, J.; Esteban, J.; Simpson, D.; Colcher, D. *Inorg. Chem.* **1986**, *25*, 2772−2781.

(31) Stimmel, J. B.; Stockstill, M. E.; Kull, F. C. *Bioconjugate Chem.* **1995**, *6*, 219−225.

(32) Brechbiel, M. W.; Gansow, O. A.; Pippin, C. G.; Rogers, R. D.; Planalp, R. P. *Inorg. Chem.* **1996**, *35*, 6343−6348.

(33) Boros, E.; Ferreira, C. L.; Cawthray, J. F.; Price, E. W.; Patrick, B. O.; Wester, D. W.; Adam, M. J.; Orvig, C. *J. Am. Chem. Soc.* **2010**, *132*, 15726−15733.

(34) Ferreiros-Martinez, R.; Esteban-Gomez, D.; Platas-Iglesias, C.; Blas, A. d.; Rodriguez-Blas, T. *Dalton Trans.* **2008**, 5754−5765.

(35) Boros, E.; Ferreira, C. L.; Patrick, B. O.; Adam, M. J.; Orvig, C. *Nucl. Med. Biol.* **2011**, *38*, 1165−1174.

(36) Platas-Iglesias, C.; Mato-Iglesias, M.; Djanashvili, K.; Muller, R. N.; Elst, L. V.; Peters, J. A.; de Blas, A.; Rodríguez-Blas, T. *Chem.—Eur. J.* **2004**, *10*, 3579−3590.

(37) Chong, H.-s.; Garmestani, K.; Ma, D.; Milenic, D. E.; Overstreet, T.; Brechbiel, M. W. *J. Med. Chem.* **2002**, *45*, 3458−3464.

(38) Wadas, T. J.; Wong, E. H.; Weisman, G. R.; Anderson, C. J. *Chem. Rev.* **2010**, *110*, 2858−2902.

(39) McMurry, T. J.; Brechbiel, M.; Kumar, K.; Gansow, O. A. *Bioconjugate Chem.* **1992**, *3*, 108−117.

(40) Liu, S.; Edwards, D. S. *Bioconjugate Chem.* **2000**, *12*, 7−34.

(41) Liu, S.; Edwards, D. In *Contrast Agents II: Optical, Ultrasound, X-ray and Radiopharmaceutical Imaging*; Krause, W., Ed.; Springer-Verlag: Berlin, Heidelberg: 2002; Vol. *222*, pp 259−278.

(42) Liu, S.; Pietryka, J.; Ellars, C. E.; Edwards, D. S. *Bioconjugate Chem.* **2002**, *13*, 902−913.

(43) Hancock, R. D. *J. Chem. Educ.* **1992**, *69*, 615−621.

(44) Maecke, H. R.; Riesen, A.; Ritter, W. *J. Nucl. Med.* **1989**, *30*, 1235−1239.

(45) Hsieh, W.-Y.; Liu, S. *Inorg. Chem.* **2004**, *43*, 6006−6014.

(46) Anderson, C. J.; Welch, M. J. *Chem. Rev.* **1999**, *99*, 2219−2234.

(47) Breeman, W. A. P.; de Jong, M.; Visser, T. J.; Erion, J. L.; Krenning, E. P. *Eur. J. Nucl. Med. Mol. Imaging* **2003**, *30*, 917−920.

(48) Wei, L.; Zhang, X.; Gallazzi, F.; Miao, Y.; Jin, X.; Brechbiel, M. W.; Xu, H.; Clifford, T.; Welch, M. J.; Lewis, J. S.; Quinn, T. P. *Nucl. Med. Biol.* **2009**, *36*, 345−354.

(49) Laverman, P.; de Vries, I. J. M.; Scharenborg, N. M.; de Boer, A.; Broekema, M.; Oyen, W. J. G.; Figdor, C. G.; Adema, G. J.; Boerman, O. C. *Nucl. Med. Biol.* **2006**, *33*, 453−458.

(50) Chakraborty, S.; Shi, J.; Kim, Y.-S.; Zhou, Y.; Jia, B.; Wang, F.; Liu, S. *Bioconjugate Chem.* **2010**, *21*, 969−978.

(51) McMurry, T. J.; Pippin, C. G.; Wu, C.; Deal, K. A.; Brechbiel, M. W.; Mirzadeh, S.; Gansow, O. A. *J. Med. Chem.* **1998**, *41*, 3546−3549.

(52) Geraldes, C. F. G. C.; Delgado, R.; Urbano, A. M.; Costa, J.; Jasanada, F.; Nepveu, F. *J. Chem. Soc., Dalton Trans.* **1995**, 327−335.
(53) Martell, A. E.; Smith, R. M. *Critical Stability Constants*; Plenum Press: New York, 1974−1989; Vol. *1*−*6*.
(54) Clarke, E. T.; Martell, A. E. *Inorg. Chim. Acta* **1991**, *190*, 37−46.
(55) Harris, W. R.; Chen, Y.; Wein, K. *Inorg. Chem.* **1994**, *33*, 4991−4998.
(56) Ando, A.; Ando, I.; Hiraki, T.; Hisada, K. *Int. J. Radiat. Appl. Instrum. B* **1989**, *16*, 57−80.
(57) Brandt, K. D.; Johnson, D. K. *Bioconjugate Chem.* **1992**, *3*, 118−125.
(58) De Sousa, M.; Carroll, A. M.; Herman, P. G.; Kerr, S.; Boulton, J.; Zalutsky, M. R. *Int. J. Nucl. Med. Biol.* **1985**, *12*, 89−96.
(59) Beamish, M. R.; Brown, E. B. *Blood* **1974**, *43*, 693−701.
(60) Van Hulle, M.; De Cremer, K.; Cornelis, R.; Lameire, N. *J. Environ. Monit.* **2001**, 3.
(61) Harris, W. R.; Messori, L. *Coord. Chem. Rev.* **2002**, *228*, 237−262.
(62) Zeng, X.; Coquière, D.; Alenda, A.; Garrier, E.; Prangé, T.; Li, Y.; Reinaud, O.; Jabin, I. *Chem.—Eur. J.* **2006**, *12*, 6393−6402.
(63) Gran, G. *Analyst* **1952**, *77*, 661−671.
(64) Duckworth, P. *Private communication.*
(65) Gans, P.; Sabatini, A.; Vacca, A. *Talanta* **1996**, *43*, 1739−1753.
(66) Baes, C. F., Jr.; Mesmer, R. E. *The Hydrolysis of Cations*; Wiley-Interscience: New York, 1976.
(67) Frisch, M. J.; et al. *Gaussian09*; Gaussian, Inc.: Wallingford CT, 2009.
(68) Lee, C.; Yang, W.; Parr, R. G. *Phys. Rev. B* **1988**, *37*, 785−789.
(69) Becke, A. D. *J. Chem. Phys.* **1993**, *98*, 5648−5652.